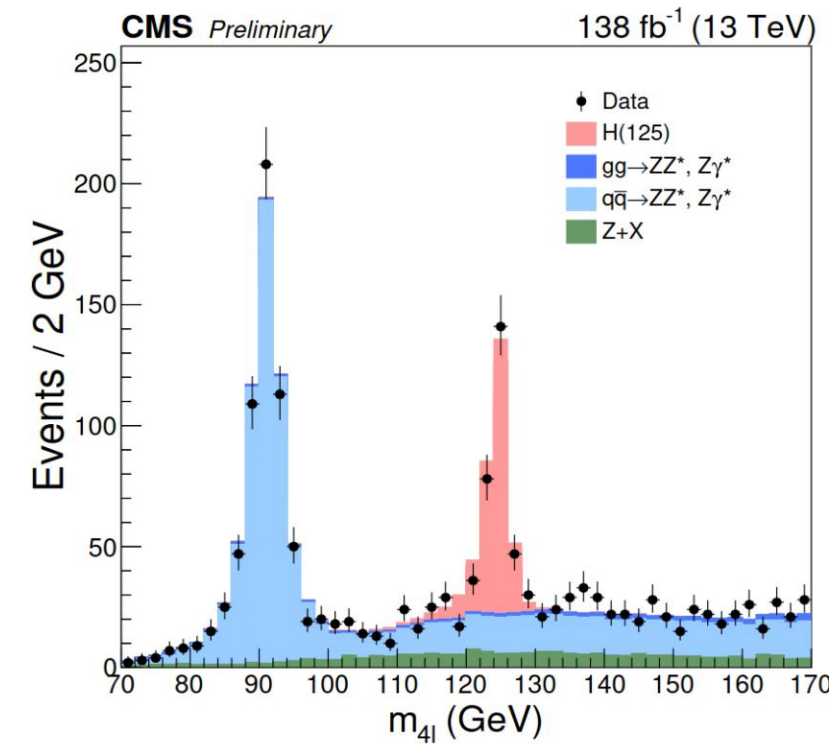


Introduction



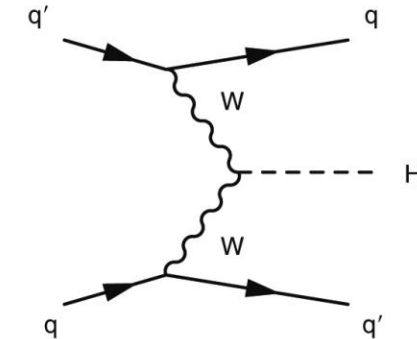
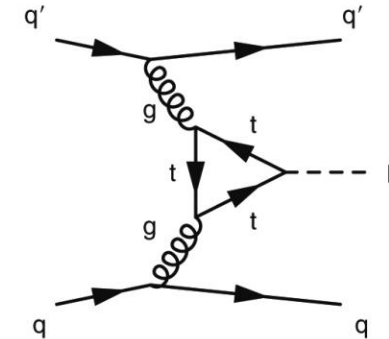
- 2012: CMS and ATLAS announce the discovery of a boson with properties compatible with those of the Higgs boson
 - Spin integer different from 1 and zero charge ($H \rightarrow \gamma\gamma$)
 - $m_H = 125, 3 \pm 0, 9 \text{ GeV}$
- 2014: Observation of disintegration $H \rightarrow \tau\tau$
- 2023: $m_H = 125, 08 \pm 0, 12 \text{ GeV}$ in the channel $H \rightarrow ZZ \rightarrow 4\ell$
- Precision measurements: couplings, decay width, spin-parity properties...
- Deviation of predictions by new physics



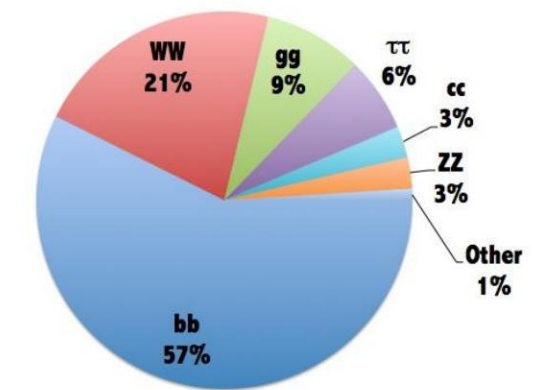
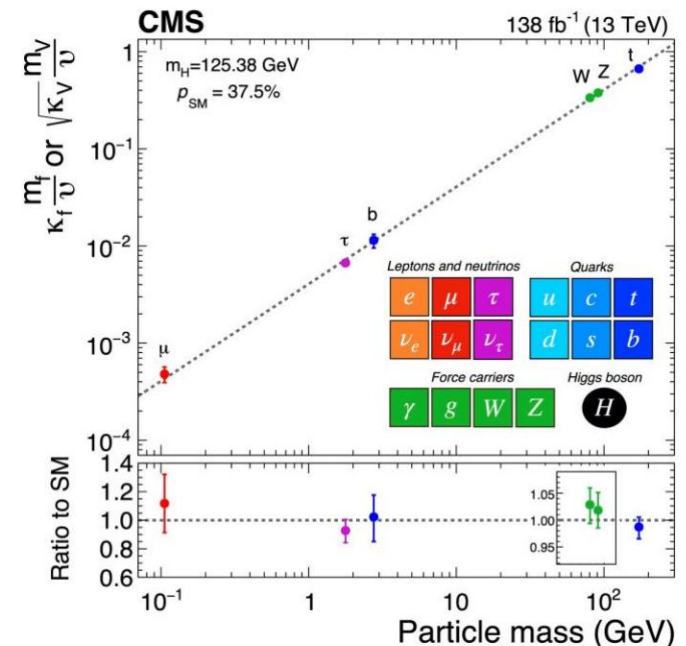
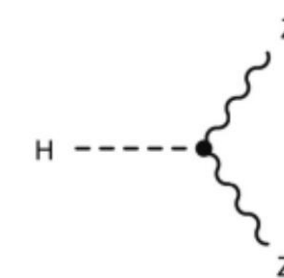
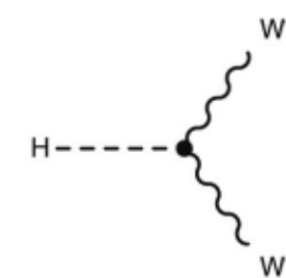
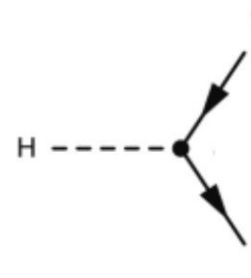
Properties of the Higgs



- Coupling to any massive particle
- Predominant production at the LHC: fusion of gluons/vector bosons



- Decay into pair of fermions/vector bosons

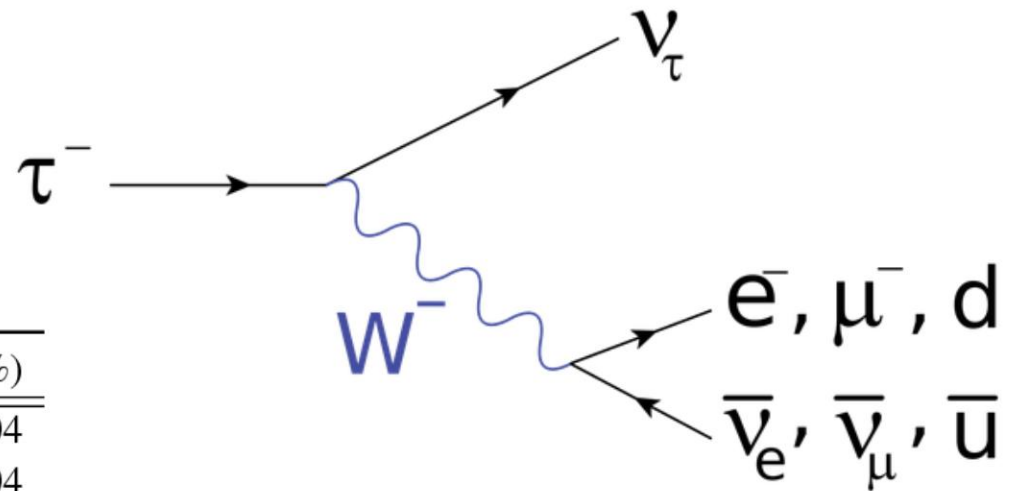


Lepton tau



- 3rd generation heavy lepton
 - Numerous couplings
 - Experimentally measurable spin

τ Decay Mode		Branching Fraction (%)
Leptonic	$\tau^\pm \rightarrow e^\pm + \bar{\nu}_e + \nu_\tau$	17.84 ± 0.04
	$\tau^\pm \rightarrow \mu^\pm + \bar{\nu}_\mu + \nu_\tau$	17.41 ± 0.04
Hadronic One-prong	$\tau^\pm \rightarrow \pi^\pm + (\geq 0 \pi^0) + \nu_\tau$	49.46 ± 0.10
	$\tau^\pm \rightarrow \pi^\pm + \nu_\tau$	10.83 ± 0.06
	$\tau^\pm \rightarrow \rho^\pm (\rightarrow \pi^\pm + \pi^0) + \nu_\tau$	25.52 ± 0.09
	$\tau^\pm \rightarrow a_1 (\rightarrow \pi^\pm + 2\pi^0) + \nu_\tau$	9.30 ± 0.11
	$\tau^\pm \rightarrow \pi^\pm + 3\pi^0 + \nu_\tau$	1.05 ± 0.07
	$\tau^\pm \rightarrow h^\pm + 4\pi^0 + \nu_\tau$	0.11 ± 0.04
Hadronic Three-prong	$\tau^\pm \rightarrow \pi^\pm + \pi^\mp + \pi^\pm + (\geq 0 \pi^0) + \nu_\tau$	14.57 ± 0.07
	$\tau^\pm \rightarrow \pi^\pm + \pi^\mp + \pi^\pm + \nu_\tau$	8.99 ± 0.06
	$\tau^\pm \rightarrow \pi^\pm + \pi^\mp + \pi^\pm + \pi^0 + \nu_\tau$	2.70 ± 0.08

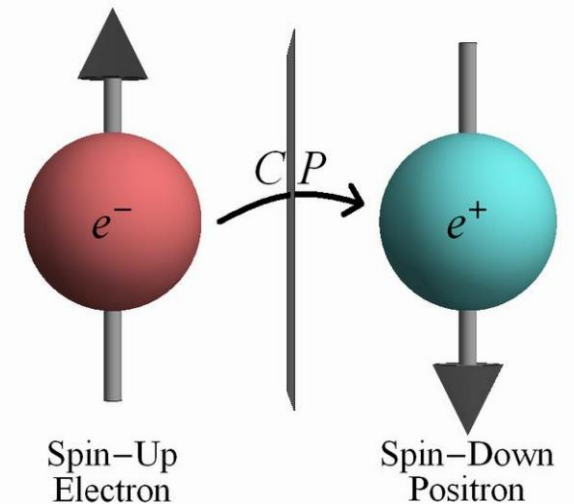
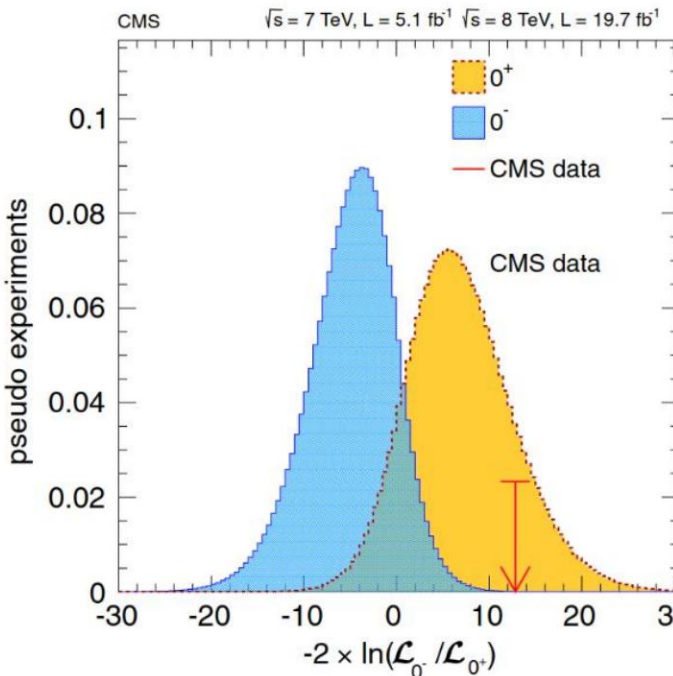


- Decay by weak interaction
 - ~33% lepton
 - ~66% hadronic

CP violation in the Higgs sector



- CP: charge-parity symmetry
- Matter-antimatter asymmetry of the Universe: existence of CP violation mechanisms
- (Too) weakly present in the standard model



- Search for new sources of violation in the Higgs sector
- Couplings to vector bosons: CP odd hypothesis excluded
- Couplings to fermions: possible violation at 1st order

CP properties of Yukawa coupling



- Each Yukawa coupling for a fermion f has the general form:

$$L_Y = -\frac{m_f \phi}{v} (\kappa_f \bar{\psi}_f \psi_f + \tilde{\kappa}_f \bar{\psi}_f i\gamma_5 \psi_f)$$

Even Odd

- The CP-odd fraction of the coupling is written:

$$f_{CP}^{Hff} = \frac{|\tilde{\kappa}_f|^2}{|\kappa_f|^2 + |\tilde{\kappa}_f|^2} = \sin^2(\alpha^{Hff})$$

- The degree of mixing of the coupling is transmitted to the pair of taus through the transverse spin correlations:

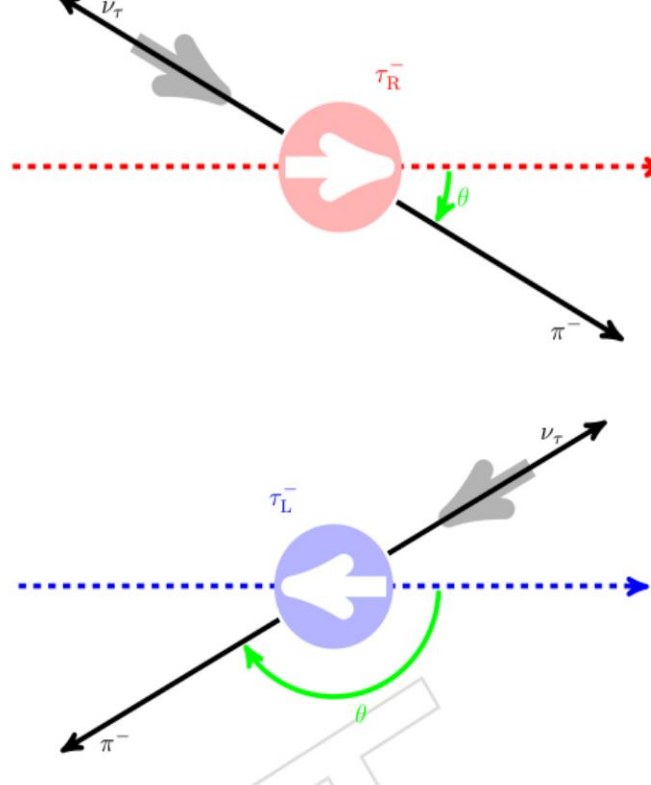
$$\Gamma(H \rightarrow \tau\tau) = \Gamma^{unpol}(1 - s_{||}^- s_{||}^+ + s_{\perp}^- R(\alpha^{H\tau\tau}) s_{\perp}^+)$$

Polarimetric vector



- Tau lepton decay rate:

$$d\Gamma = \frac{1}{2m_\tau} |\overline{M}|^2 (1 + h_\mu s^\mu) dLips$$



- $m\ddot{\gamma}$: tau mass
- M : matrix element
- h : polarimetric vector
- s : tau spin

- Polarimetric vector $\ddot{\gamma}$ most probable direction of the spin of the tau lepton
 - $\tau \rightarrow \pi\nu$: $h\ddot{\gamma}$ direction of the neutrino
 - For spin 1 resonances: more complex models
- Requires complete reconstruction of the tau lepton quadruple momentum

Definition of a CP observable

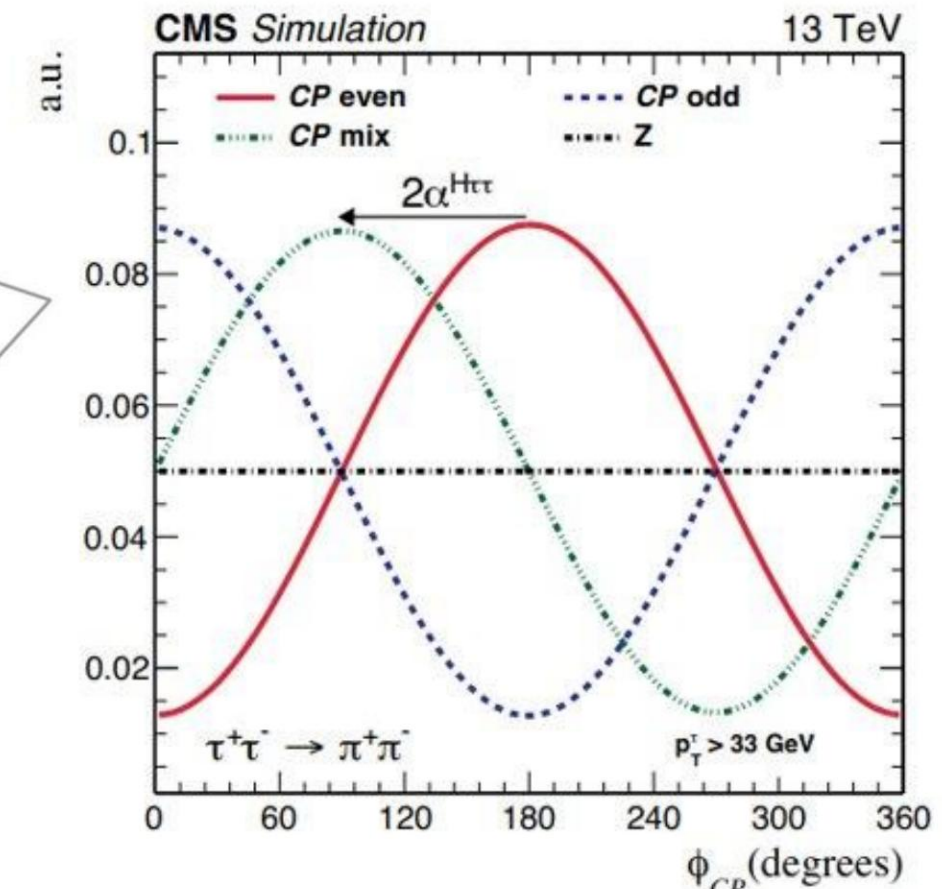
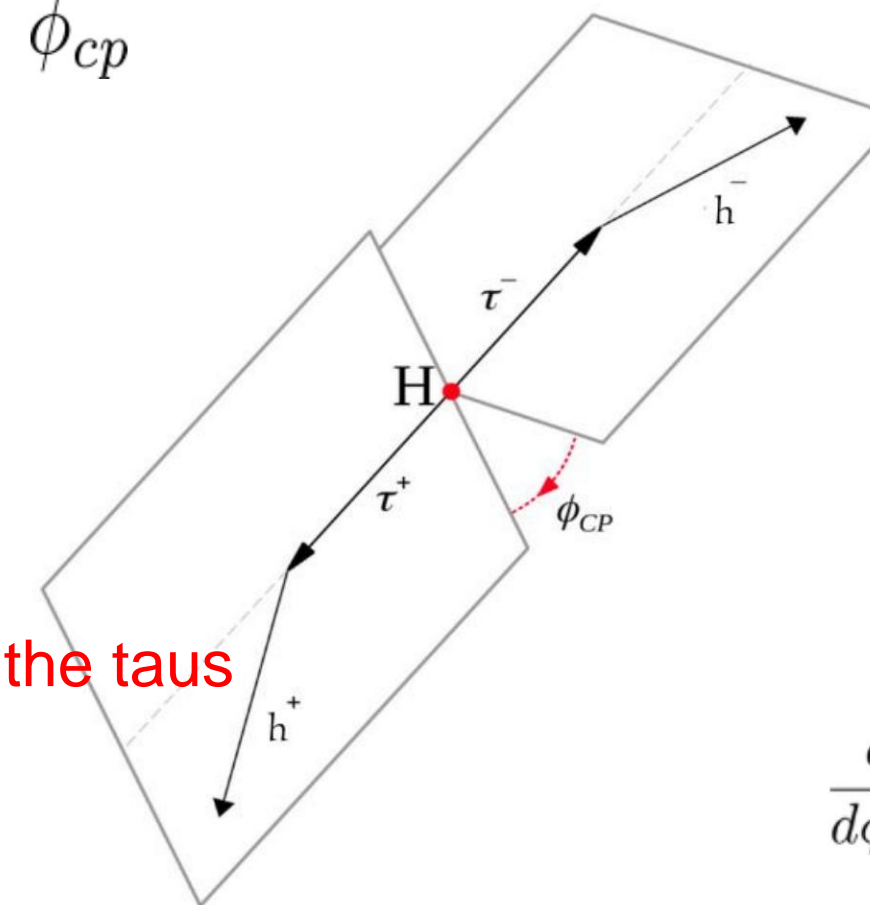


- Angle between the transverse components of the tau spin in the rest frame of the Higgs boson:

$$\phi_{CP}$$

- Use of polarimetric vector and the direction of the tau lepton:

reconstruction of the taus

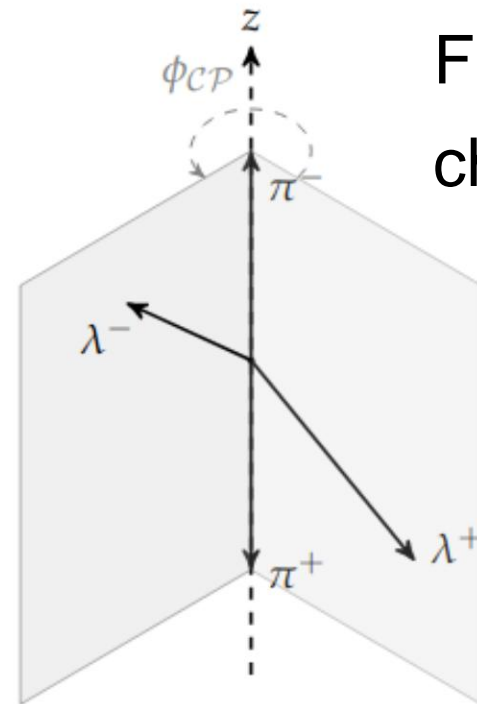


$$\frac{d\Gamma}{d\phi_{CP}}(H \rightarrow \tau\tau) \propto \text{const} - \cos(\phi_{CP} - 2\alpha^{H\tau\tau})$$

Experimental measurement



- Approximation of ϕ_{CP} from visible decay products

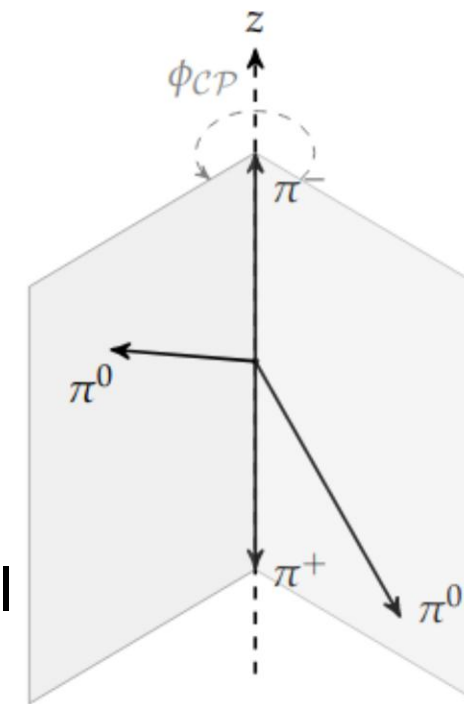


Impact parameter

$$\tau \rightarrow \pi, \mu, e$$

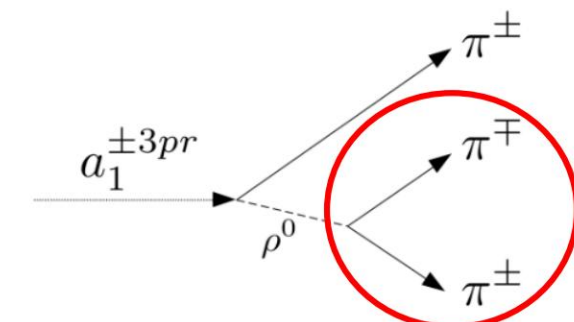
Final states of a charged particle

Final states with several particles including at least one charged



Neutral pion

$$\tau \rightarrow \rho, a_1$$

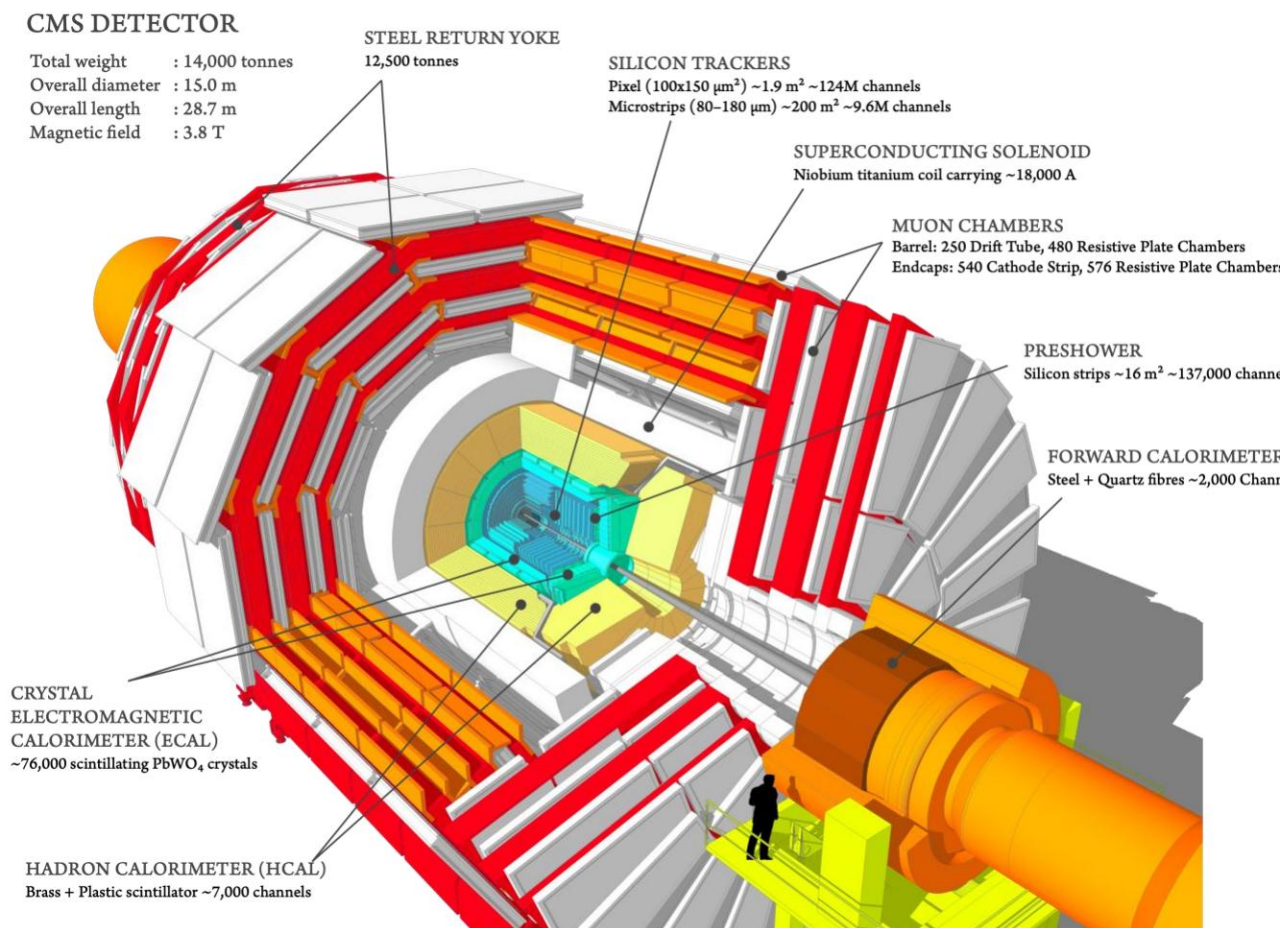


(decay plane)

Compact Muon Solenoid

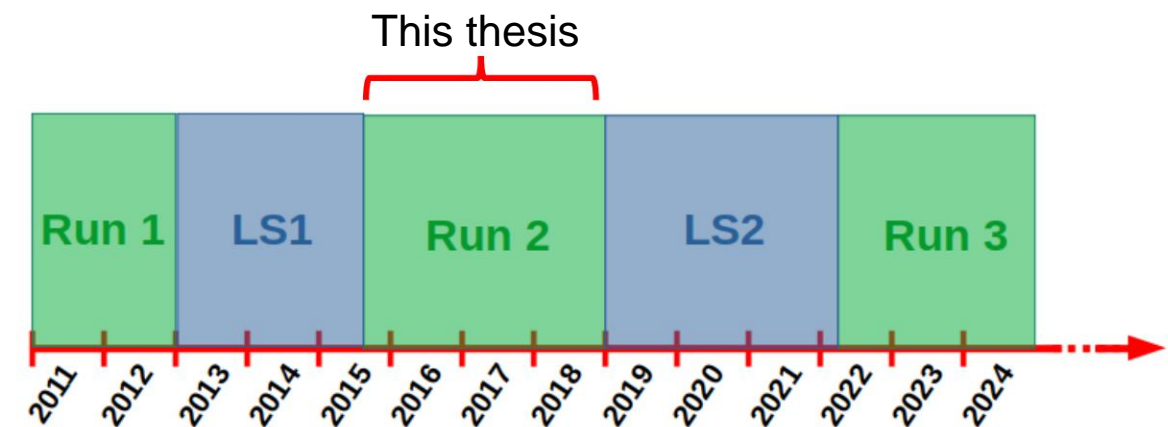


- General layer detector



- Run 2: pp collisions at 13 TeV delivered by the Large Hadron Collider (+ Pb-Pb collisions)

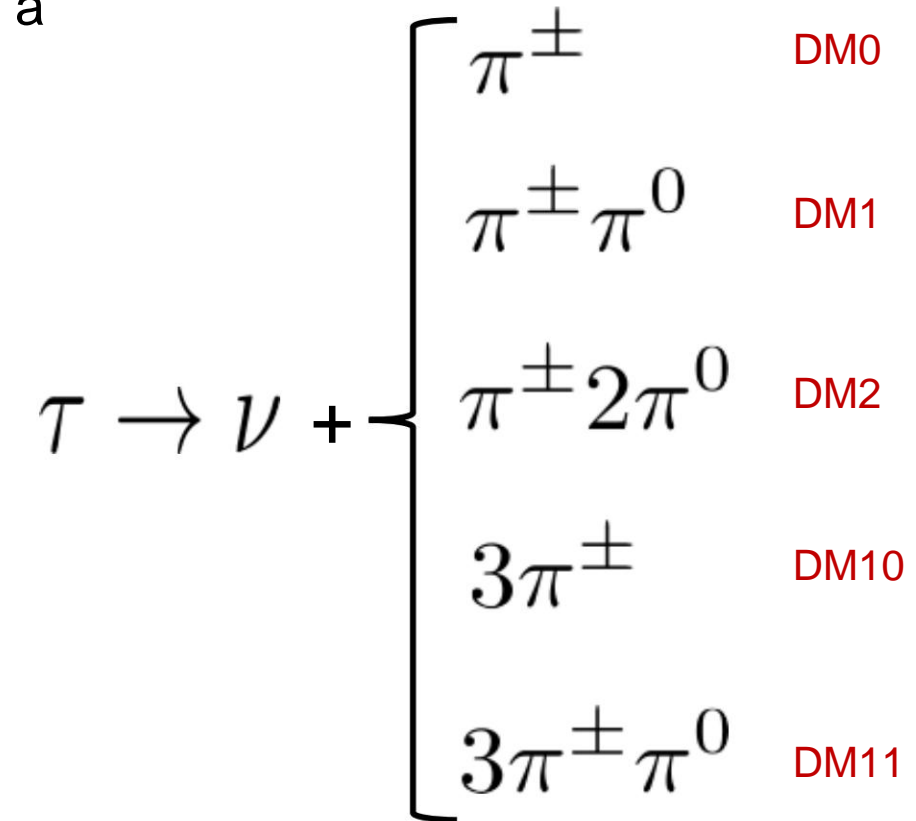
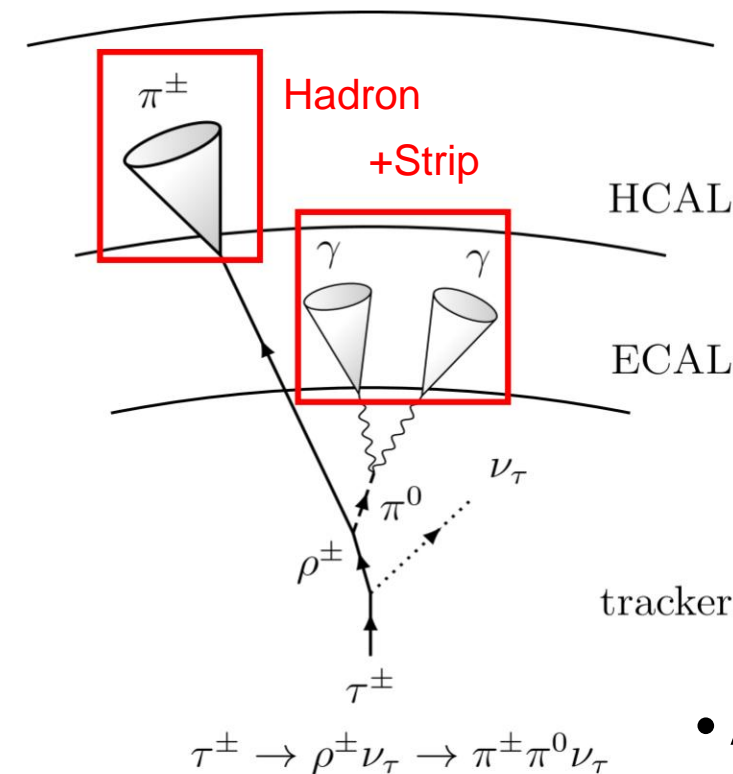
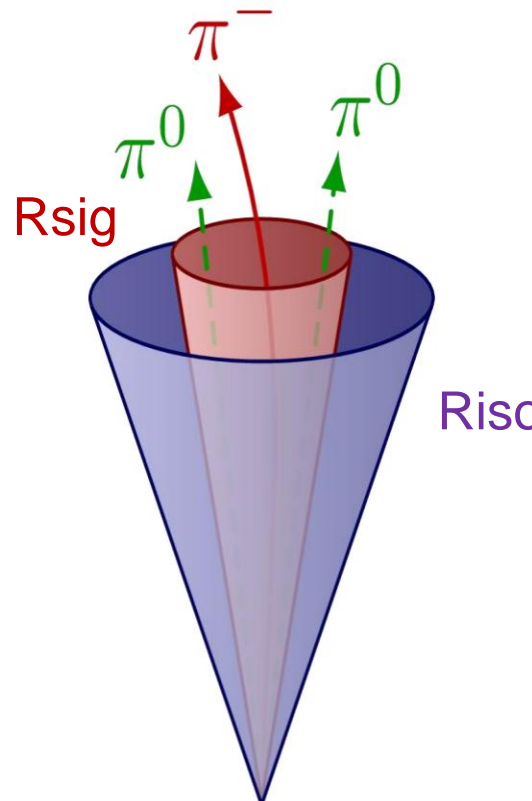
- Run 3: 13.6 TeV and increase in instantaneous luminosity





Reconstruction of taus in CMS

- HPS algorithm: association of neutral and charged hadrons within a cone • Centered on the charged hadron with the highest pT within a jet • Isolation: $R = 0.4$ • Signal: $R = 2.8/pT$ (iso)



- Assignment of a decay mode



Identification of taus in CMS

- Several objects causing identification errors:

- Collimated jets
- Electrons and bremsstrahlung $(\tau \rightarrow \pi\pi^0)$
- Muons $(\tau \rightarrow \pi)$

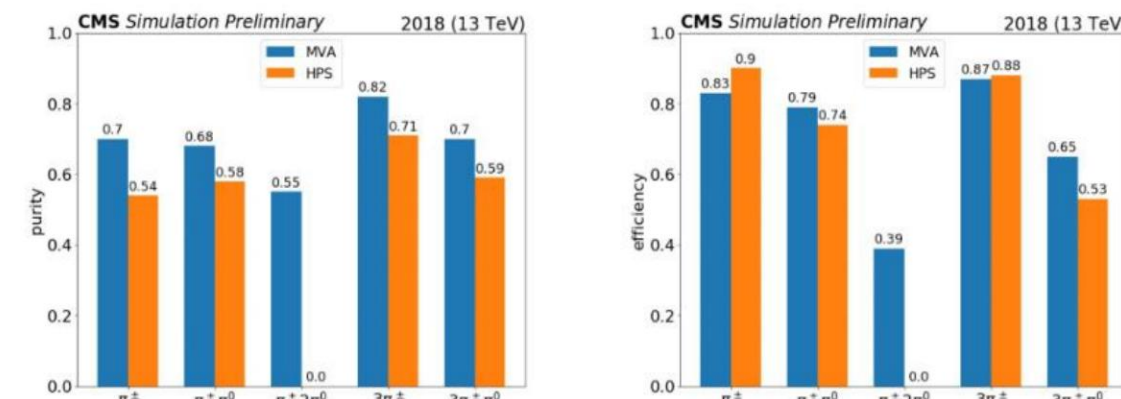
- DeepTau: deep multiclass neural network

- 4 classes: e, μ, jet, τ

$$D_\alpha(y) = \frac{y_\tau}{y_\tau + y_\alpha}, \quad \alpha = e, \mu, jet$$

- MVA-DM: second determination of the decay mode from the HPS-DM

- Optimized purity



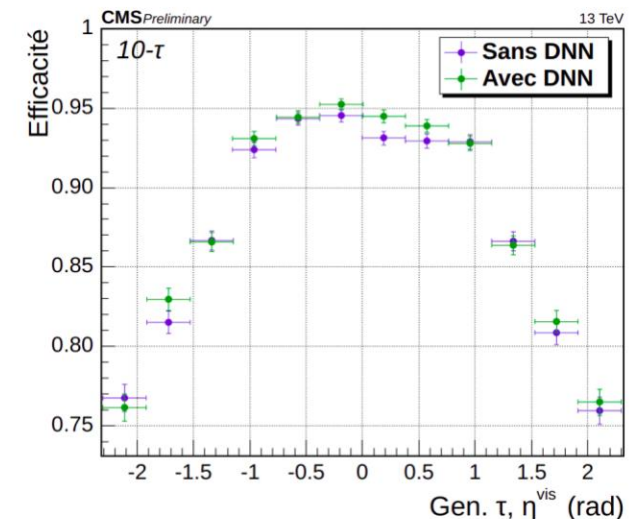
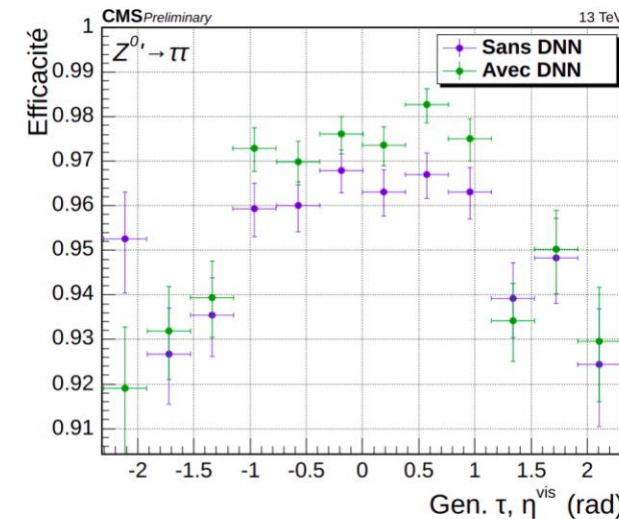
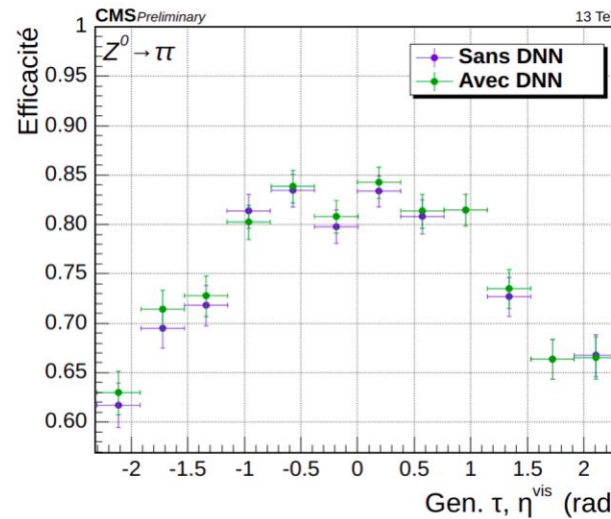
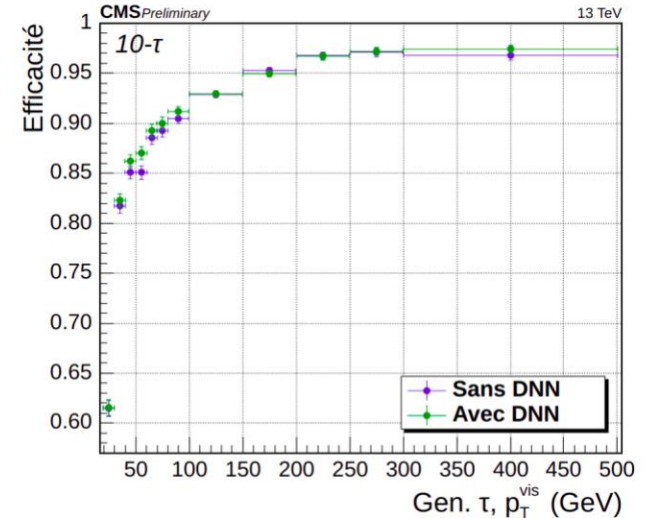
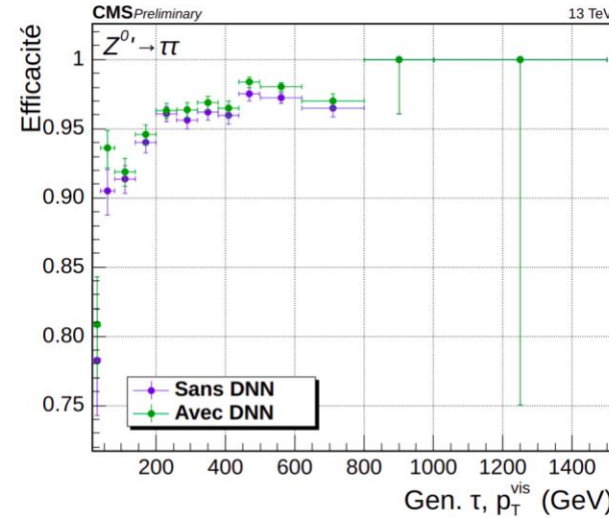
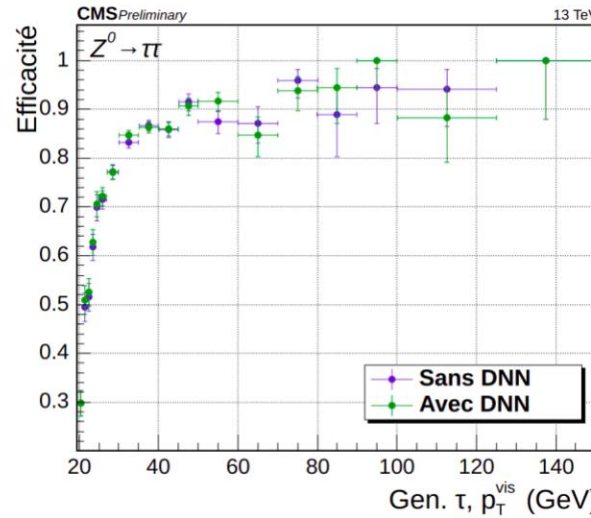


Tau reconstruction efficiency

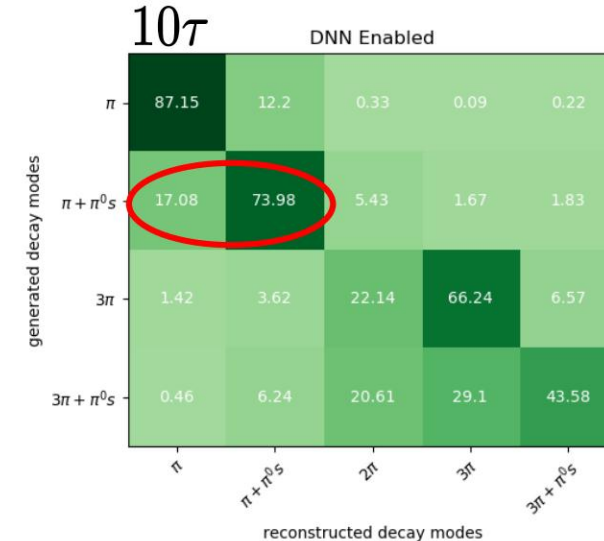
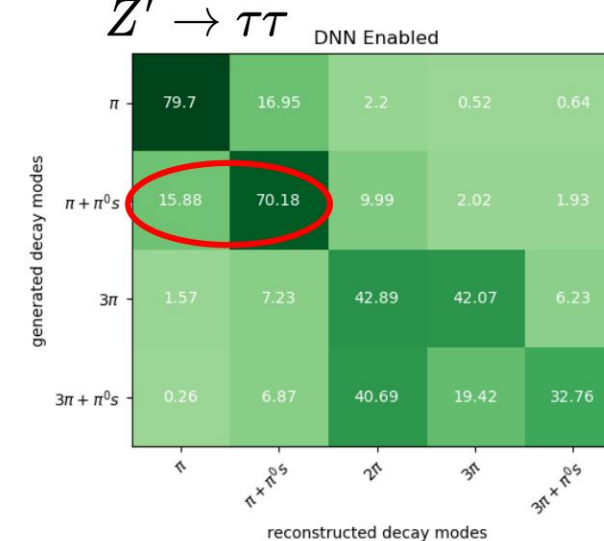
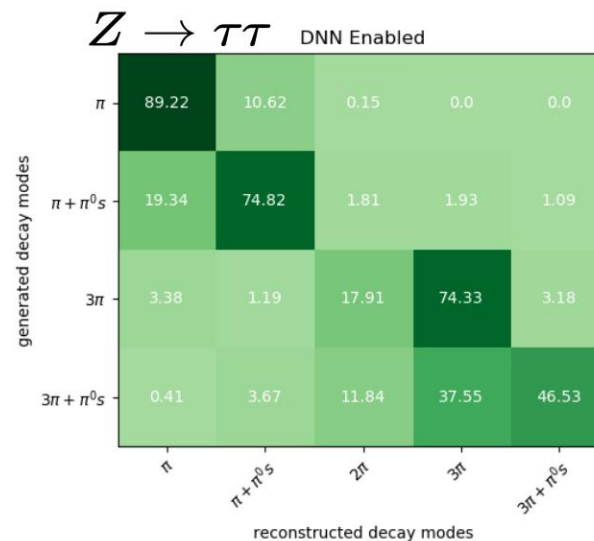
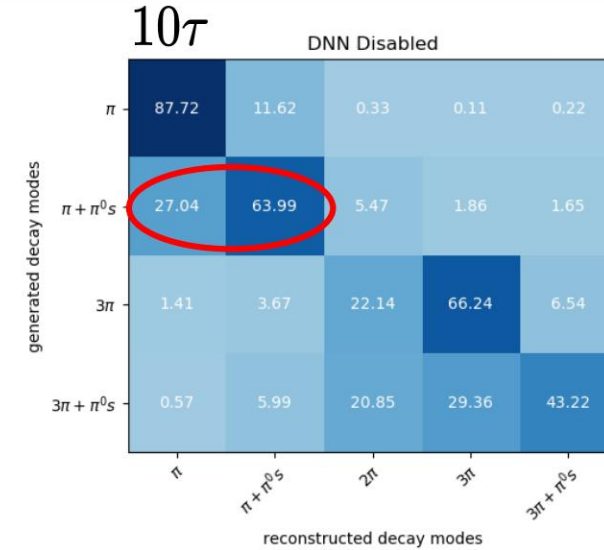
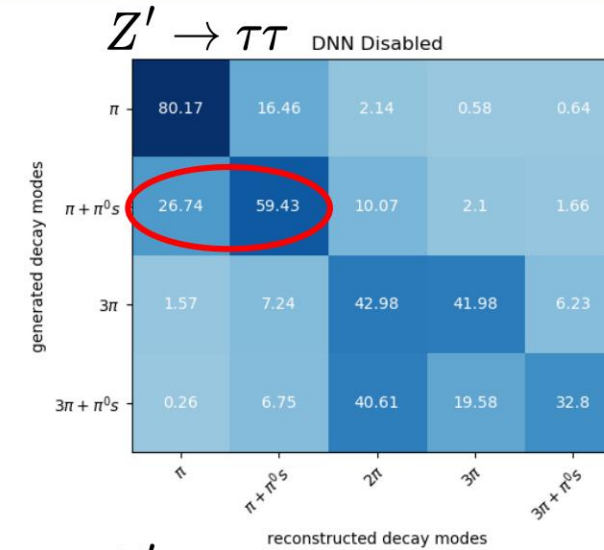
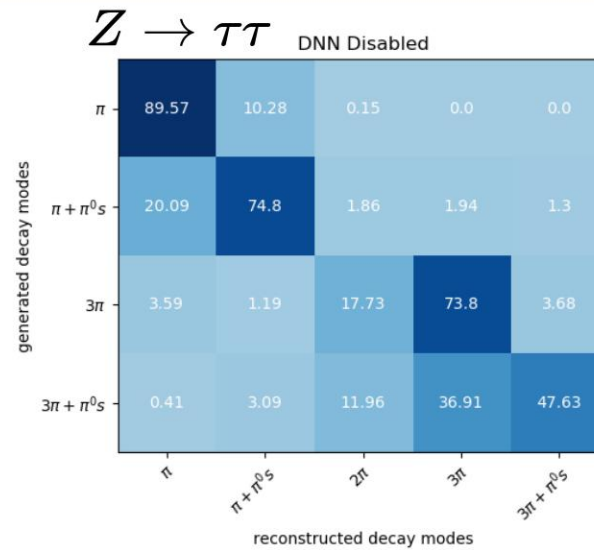
- Between Run 1 and Run 2: 5-10% loss of HPS efficiency on DMs $\tau_h \rightarrow \pi^\pm \pi^0 s$
 - Attributed to the “*single-track*” identification of converted photons using a network of neurons during Run 2
 - Increase in the rate of false photons and loss of candidate hadrons for tau reconstruction
- Run 3: retraining the neural network
 - Verification of the impact of its use on HPS performance
 - Three samples: $Z \rightarrow \tau\tau$, $Z'(1500) \rightarrow \tau\tau$, 10τ
- Efficiency defined by the ratio of the number of taus reconstructed by HPS and the number of taus generated independently of the decay mode



Tau reconstruction efficiency



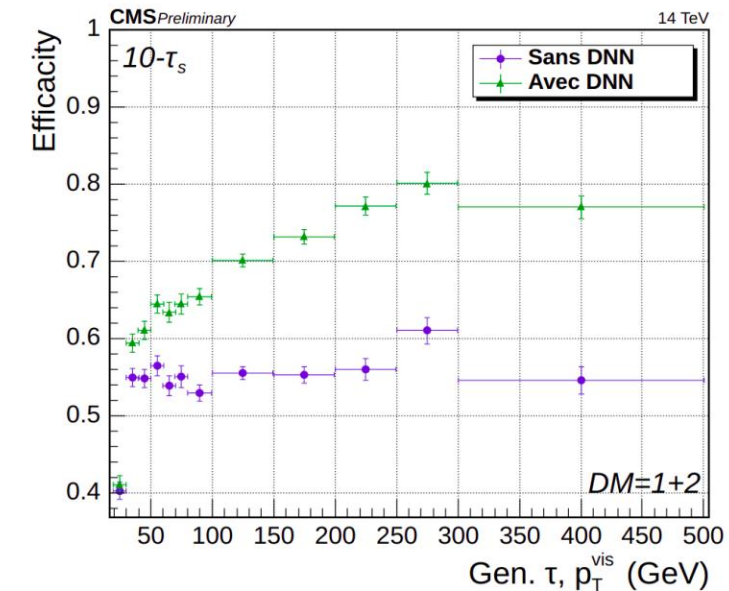
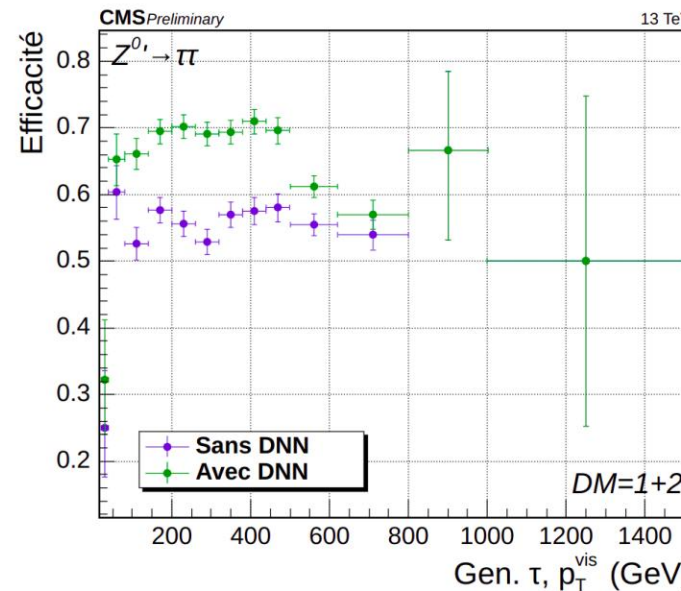
Tau reconstruction efficiency





Tau reconstruction efficiency

- Improvement in the effectiveness of DM 1 and 2 at high pT



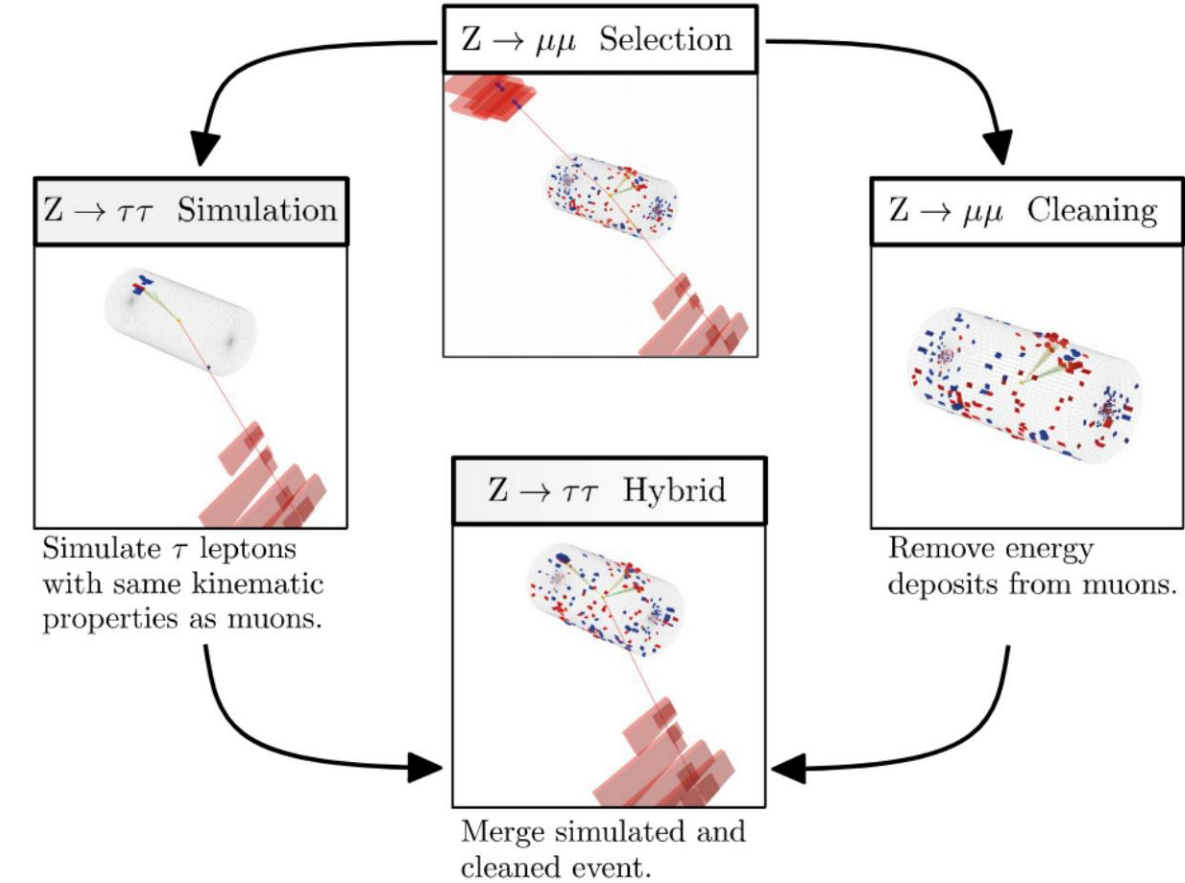
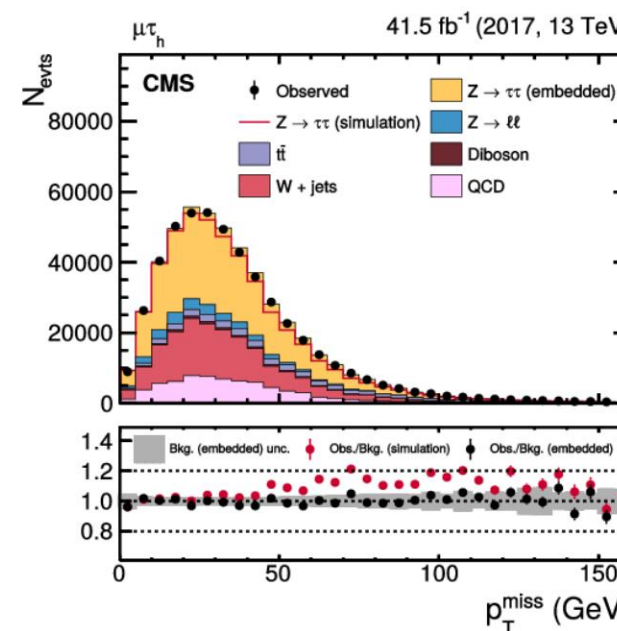
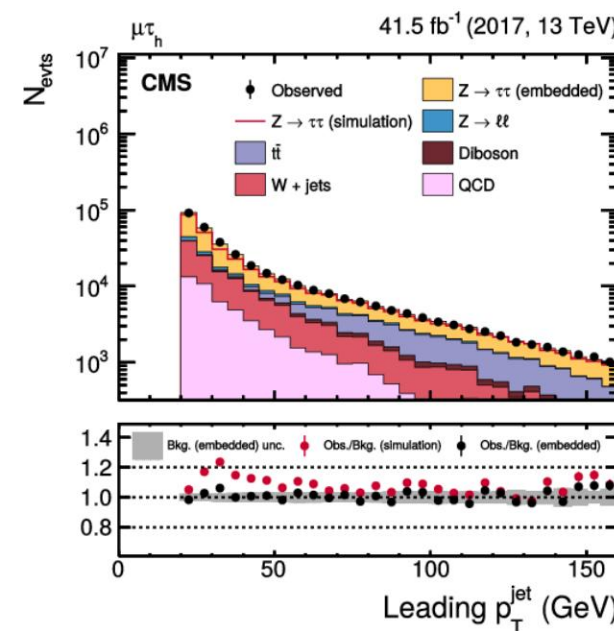
- Stable tau reconstruction performance for Run 3: inclusion of the algorithm in the CMS software



Embedding

- Estimation of background noise
 - Hybrid data/MC events
 - Better overall description of the event

$$Z \rightarrow \tau\tau$$

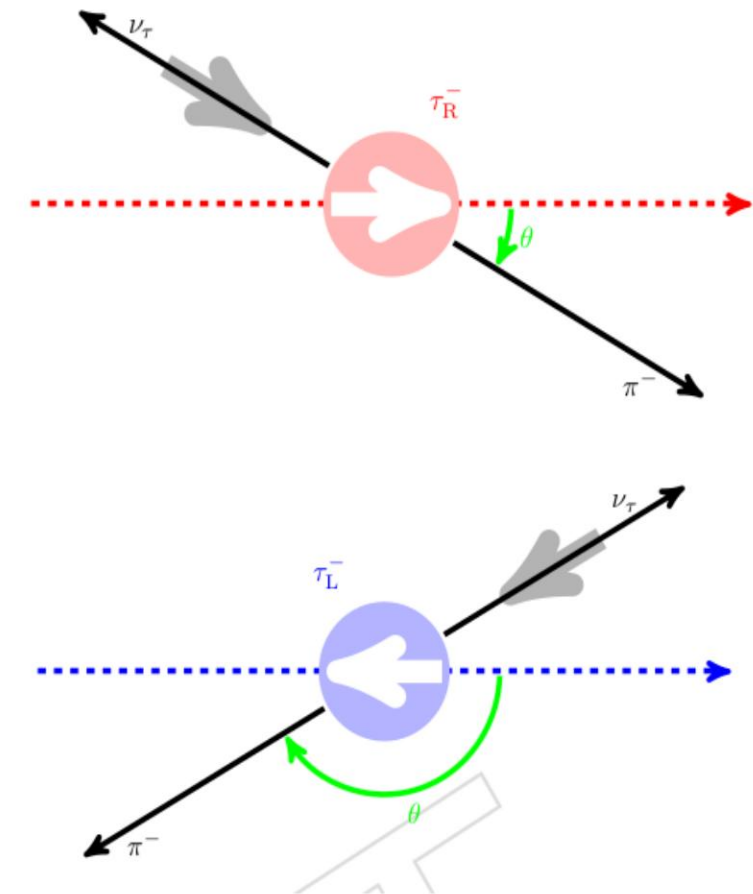
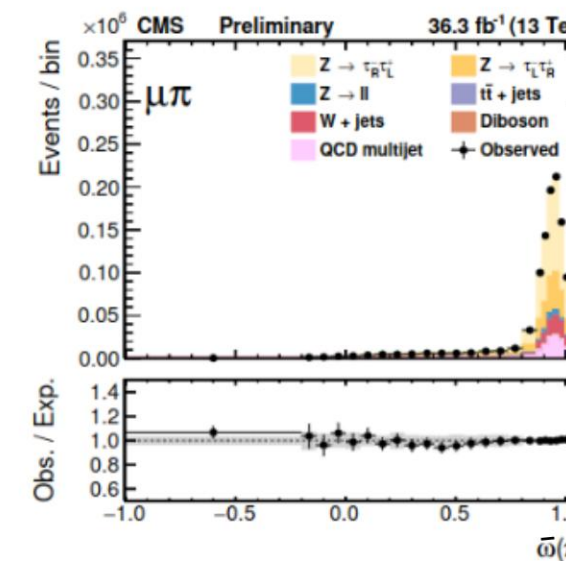
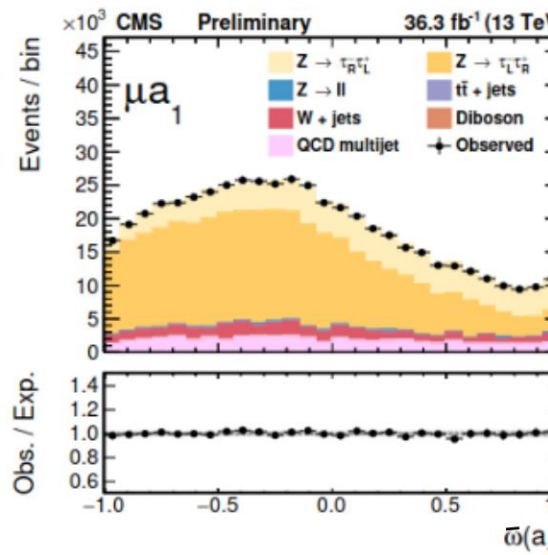




Optimal spin variables

- Angle between the polarimetric vector and the direction of the tau in its reference frame at rest: $\bar{\omega}$
- $\tau \rightarrow \pi \nu$: $\bar{\omega} = \theta$
- Sensitive to tau lepton polarization

$$\frac{d\Gamma}{d \cos \bar{\omega}} \propto \frac{1}{2} (1 + P_\tau \cos \bar{\omega})$$



Optimal spin variables



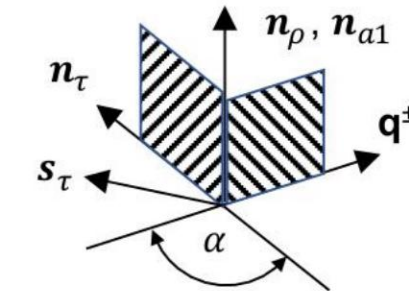
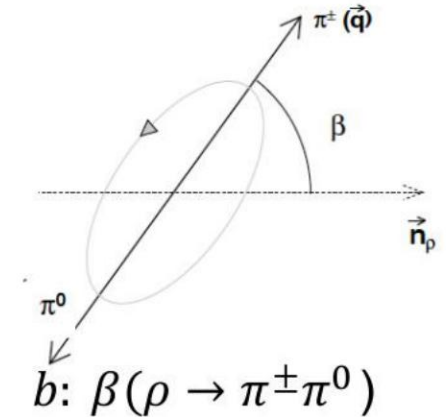
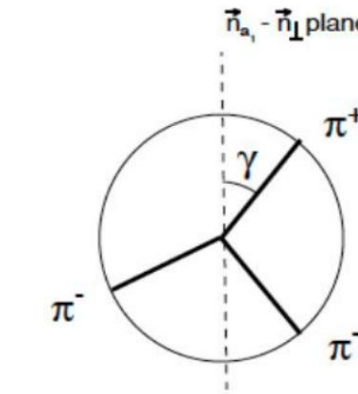
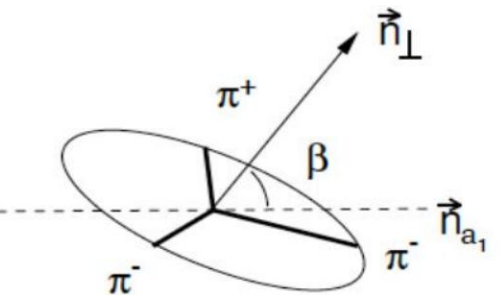
- More complex definition for spin 1 resonances

- Exploitation of spin correlations:

$$\overline{\Omega} = \frac{\overline{\omega}_1 + \overline{\omega}_2}{1 + \overline{\omega}_1 \cdot \overline{\omega}_2}.$$

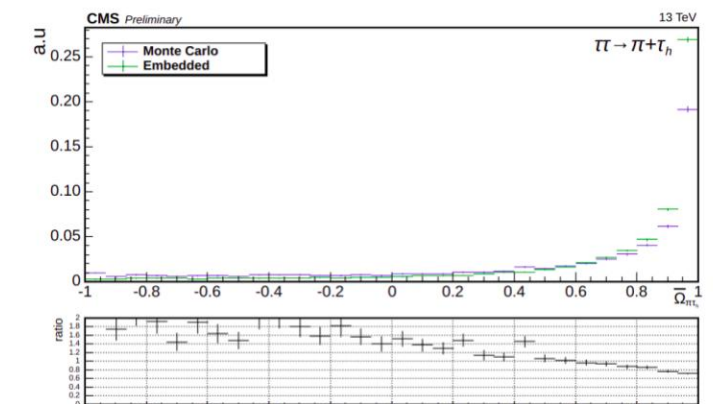
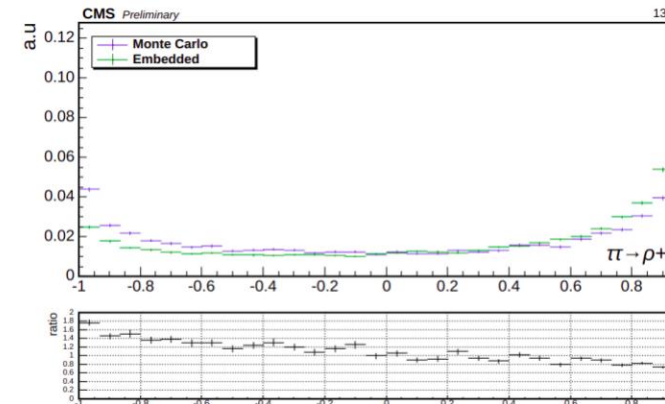
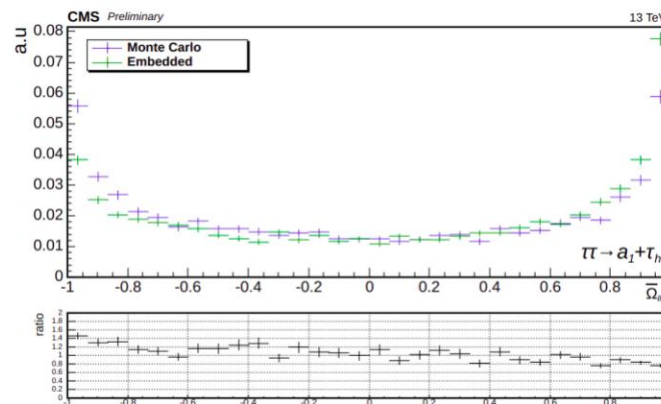
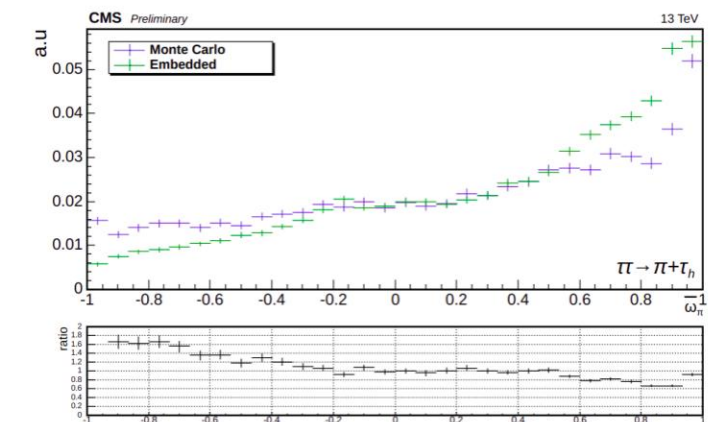
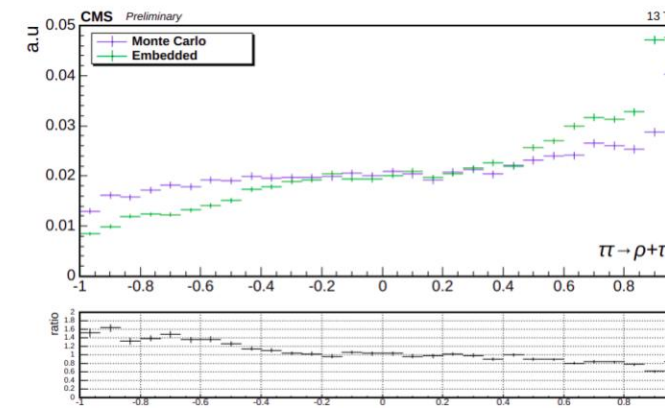
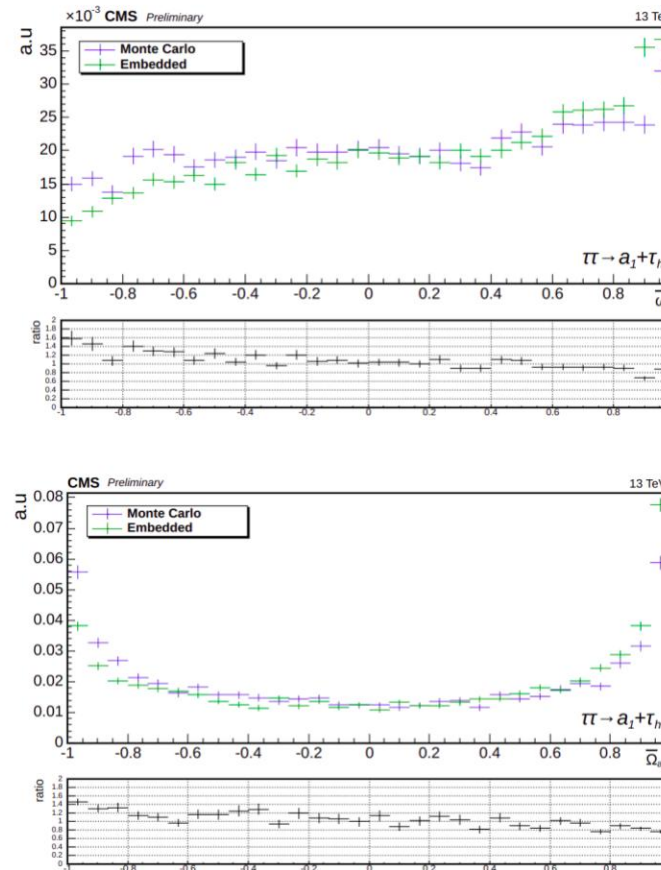
- First study of optimal spin variables in *embedded samples*

- MC/embed comparison
- Search for a potential propagation error of spin effects during simulation

a: $\alpha(\tau \rightarrow \rho, a_1)$ b: $\beta(\rho \rightarrow \pi^\pm \pi^0)$ c: $\gamma(a_1 \rightarrow \pi^+ \pi^- \pi^0)$ d: $\beta(a_1 \rightarrow \pi^+ \pi^- \pi^0)$



Optimal spin variables

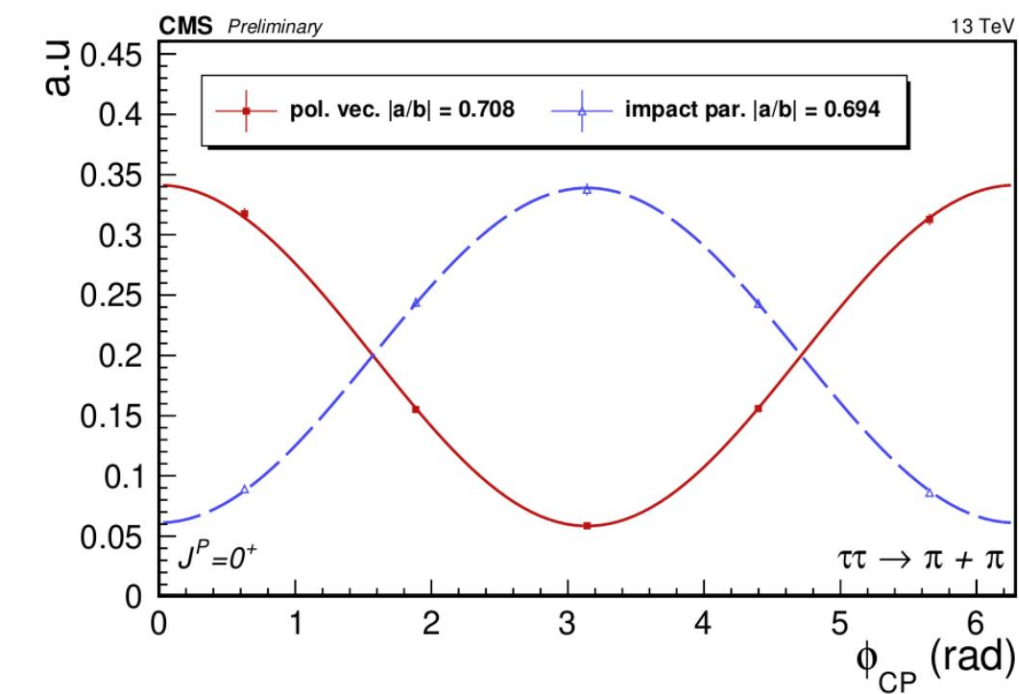


- No significant effects that could indicate a spin propagation error
- Alignment between simulated and real detector possibly causing disagreements observed

Polarimetric vector performance



- Comparison of methods
 - $\tau \rightarrow \rho, a_1$: neutral pion vs polarimetric vector
 - $\tau \rightarrow \pi$: impact parameter vs polarimetric vector
- Adjustment of the distributions ϕ_{cp} :
 - of $f(x) = a * \cos(x) + b$
- Measurement of oscillation amplitude: $|a/b|$
 - Better separation = better sensitivity
- Phase shift between methods of conventional origin

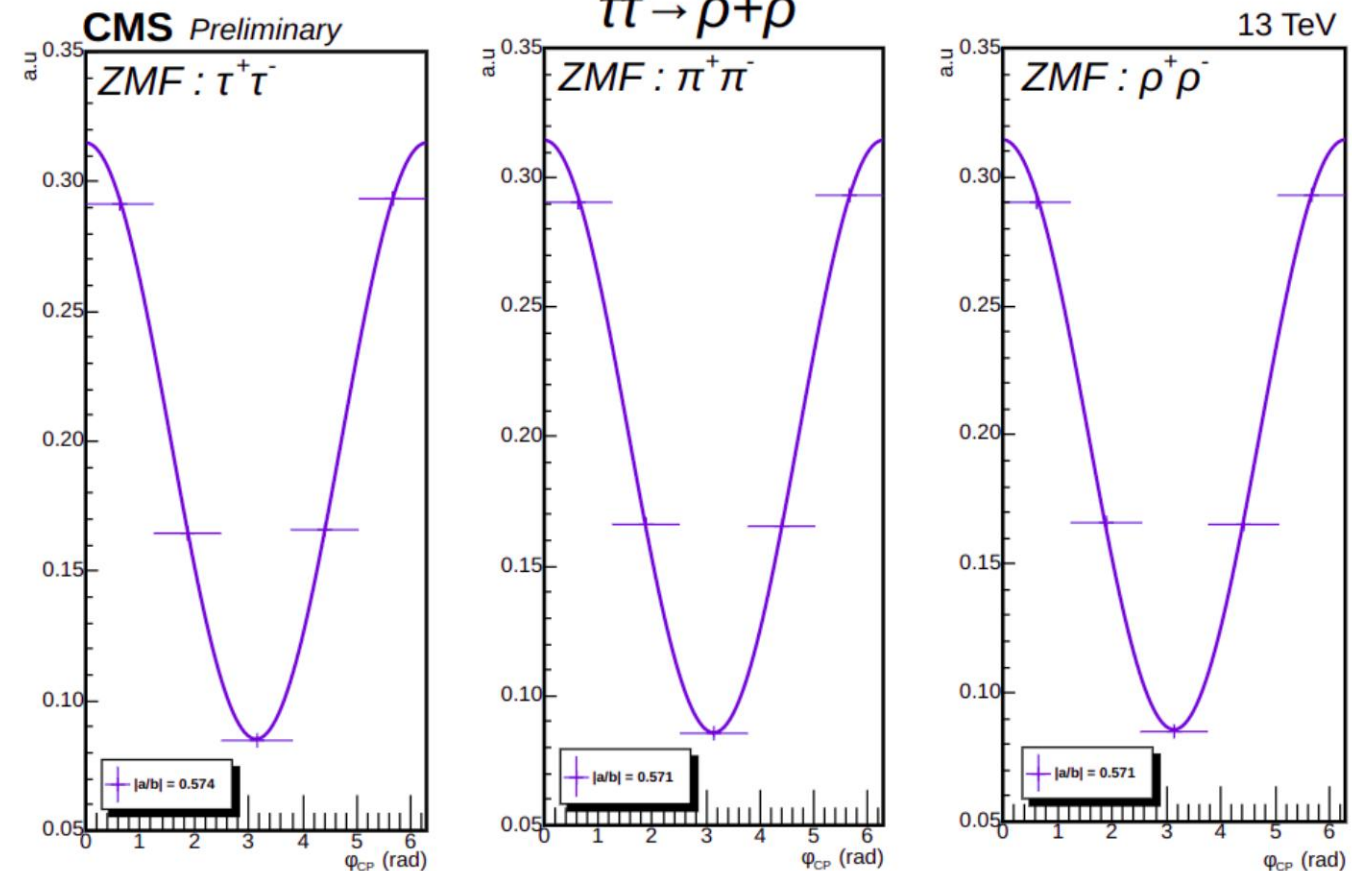




Polarimetric vector performance

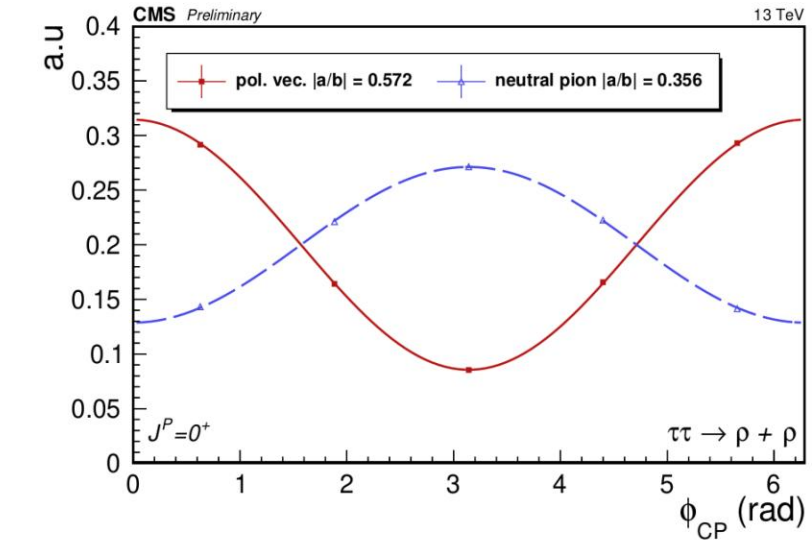
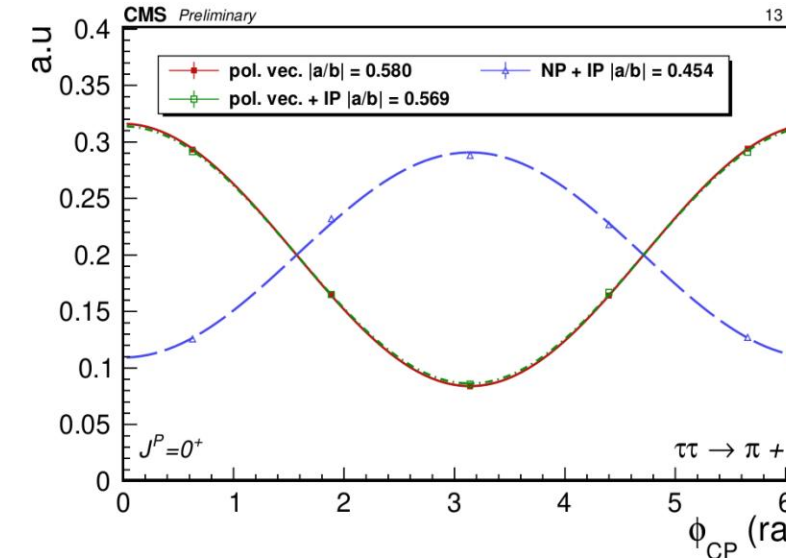
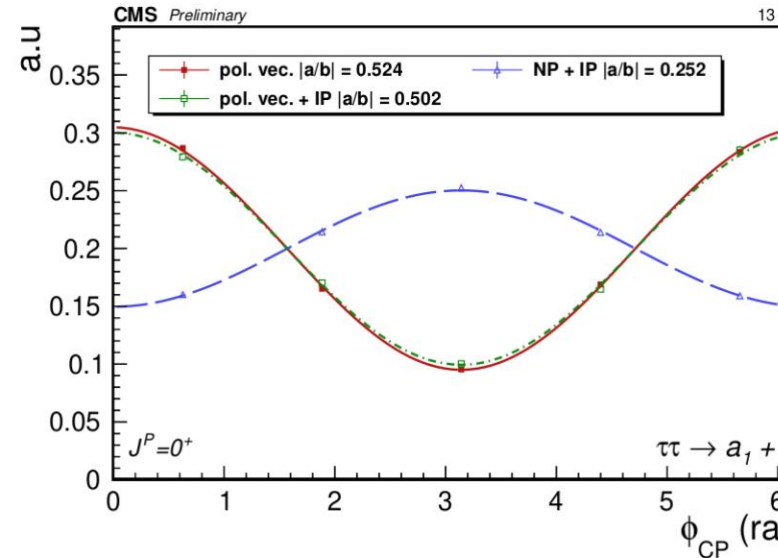
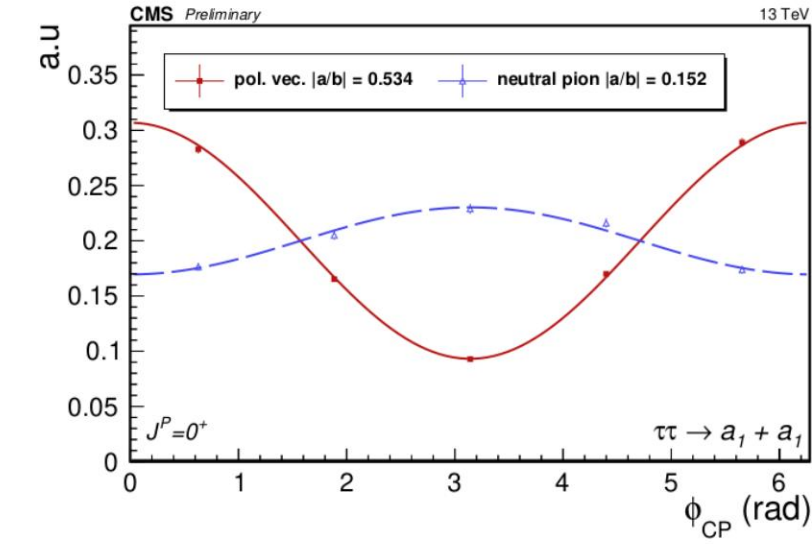
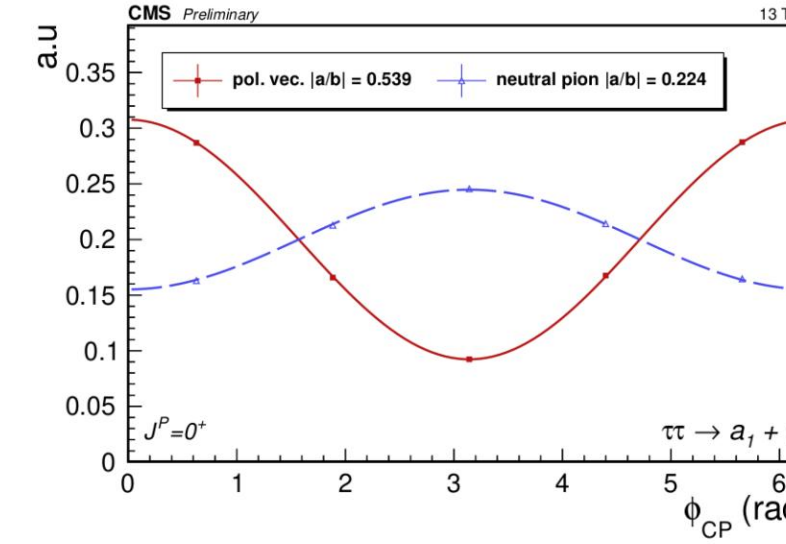
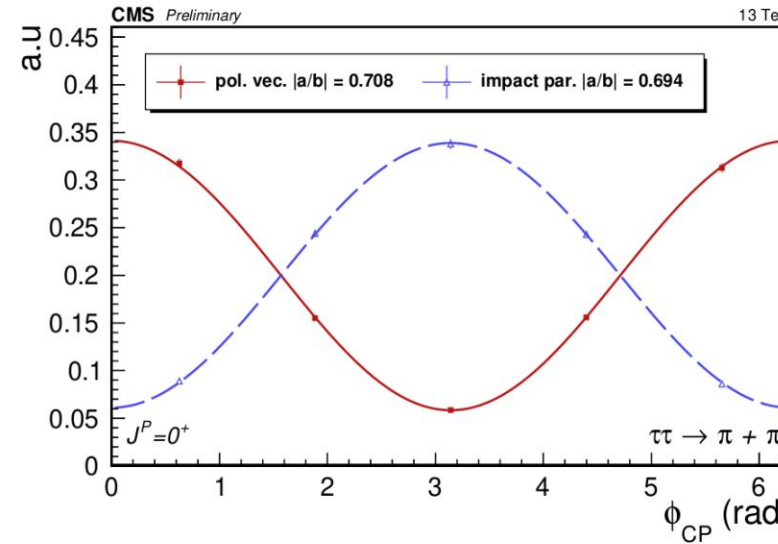
- No impact in the choice of the generator calculation benchmark

ϕ_{cp} at the level



Polarimetric vector performance

generator level

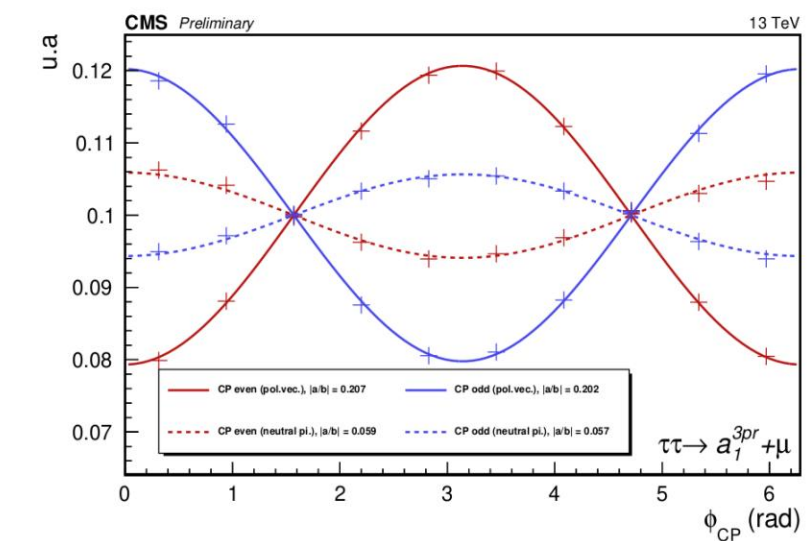
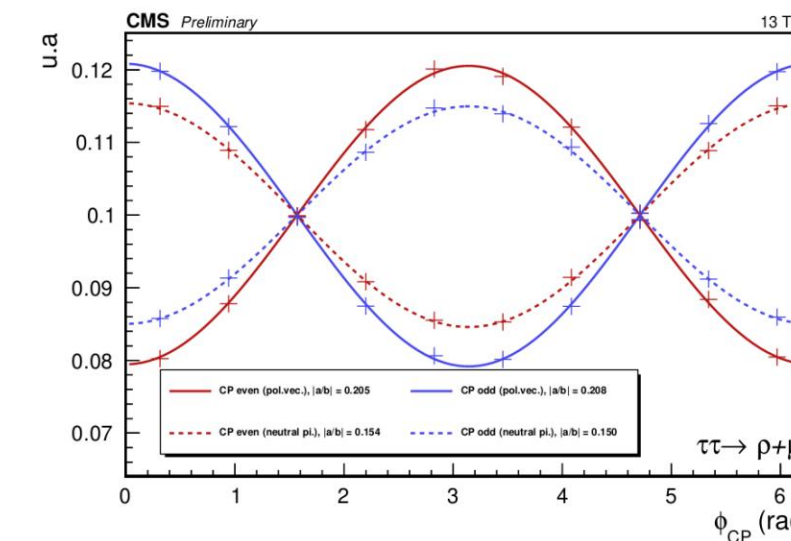
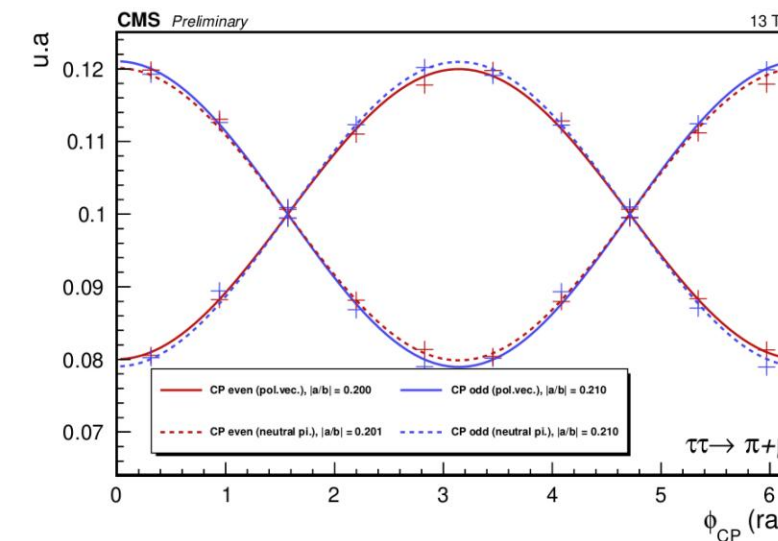


Polarimetric vector performance

generator level



- Comparison of methods
 - $\tau \rightarrow \rho, a_1$: neutral pion < polarimetric vector
 - $\tau \rightarrow \pi$: impact parameter = polarimetric vector
- Same conclusion for semi-leptonic channels
- Reconstructed level: impact parameter to be preferred



Reconstruction of the tau pulse

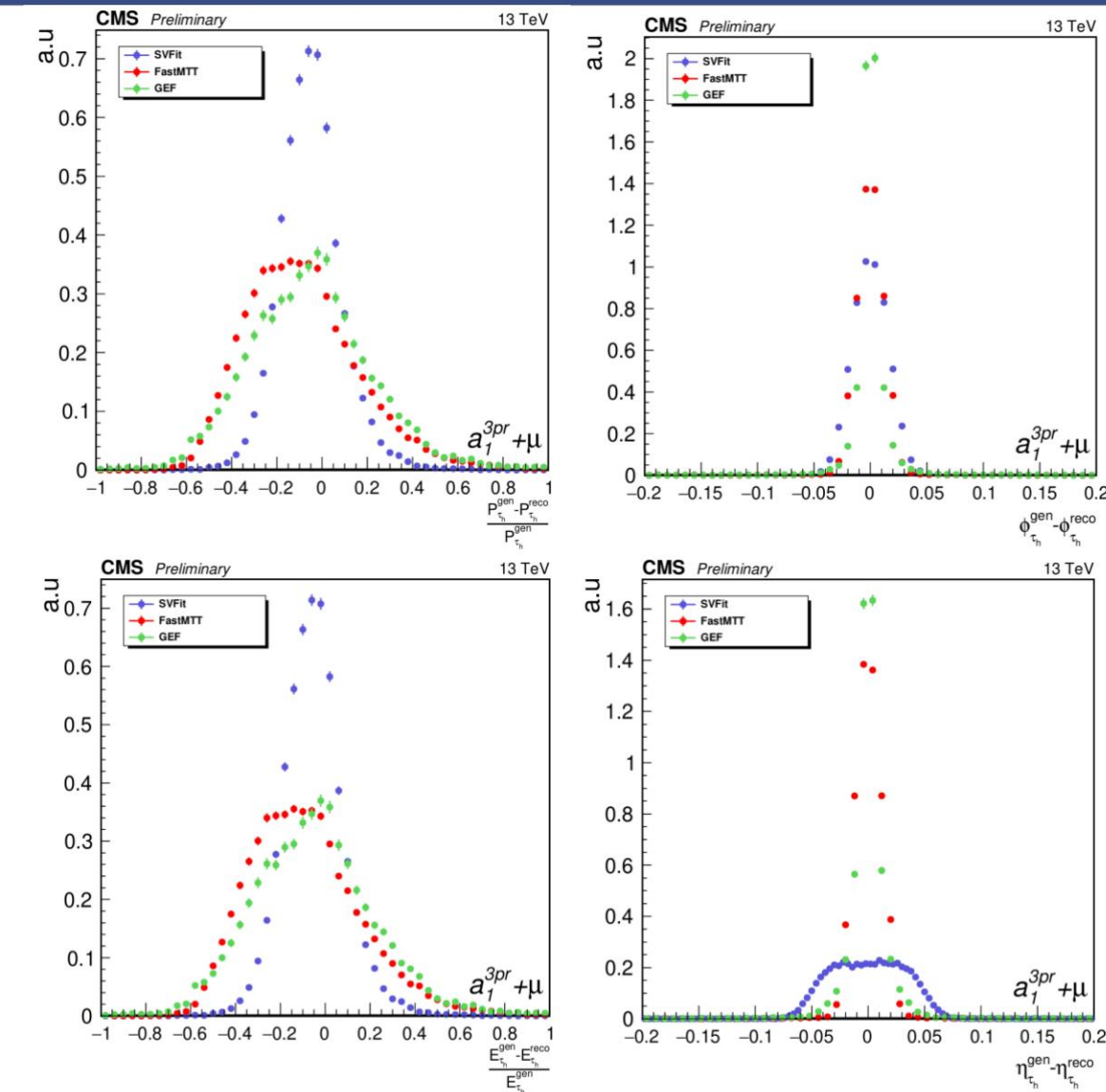


- SVFit: reconstruction of the di-tau mass for Higgs analyzes
 - Dynamic likelihood maximization method

$$P(M_{\tau\tau}) = \int \delta(M_{\tau\tau} - M_{\tau\tau}(\vec{y}, \vec{a})) p(\vec{x}|\vec{y}, \vec{a}) d\vec{a}.$$

- $M_{\tau\tau}$: masse du système di-tau
- \vec{a} : paramètres cinématiques du système di-tau
- \vec{x} : MET observée
- \vec{y} : impulsion des produits visibles

- FastMTT: SVFit with reduced phase space , collinear approximation
- GEF: kinematic adjustment in channels a_1+X



Global Event Fit



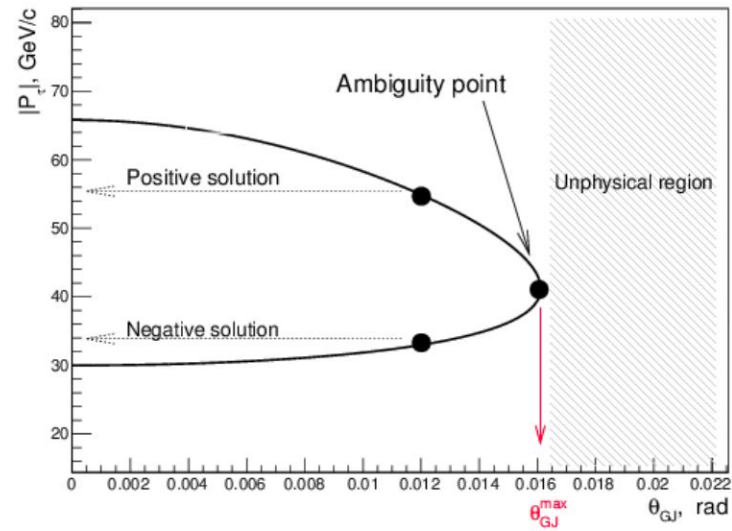
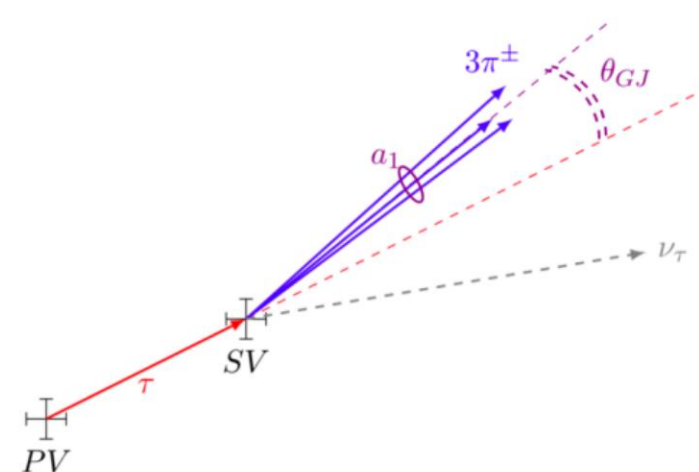
- Reconstruction of events on channels a_1+X
 - Reconstruction of the management of
 - Measurement of the first pulse
 - Kinematic adjustment of the pair from a set of constraints

$$\vec{H} = \begin{cases} M_{\tau\tau} - M_{Z/H} &= 0 \\ p_z - |\vec{p}_2| \cos \theta_2 &= 0, \end{cases}$$

$$\vec{f} = \begin{cases} p_x^{\tau_1} + p_x^{\tau_2} - p_x^{a_1} - p_x^{\text{vis}_2} - MET_x &= 0 \\ p_y^{\tau_1} + p_y^{\tau_2} - p_y^{a_1} - p_y^{\text{vis}_2} - MET_y &= 0. \end{cases}$$

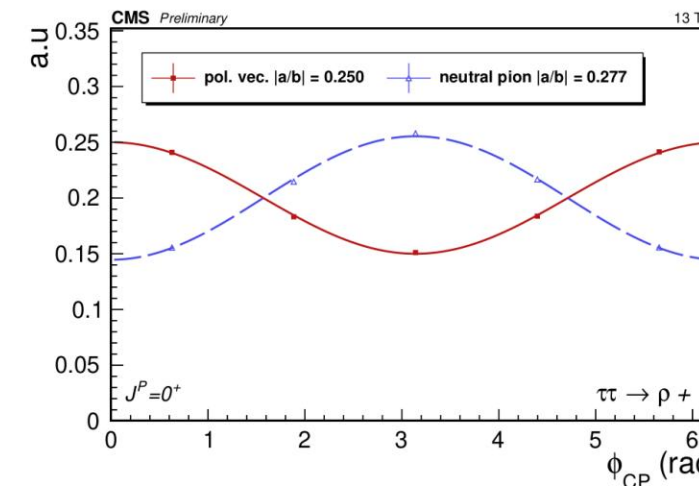
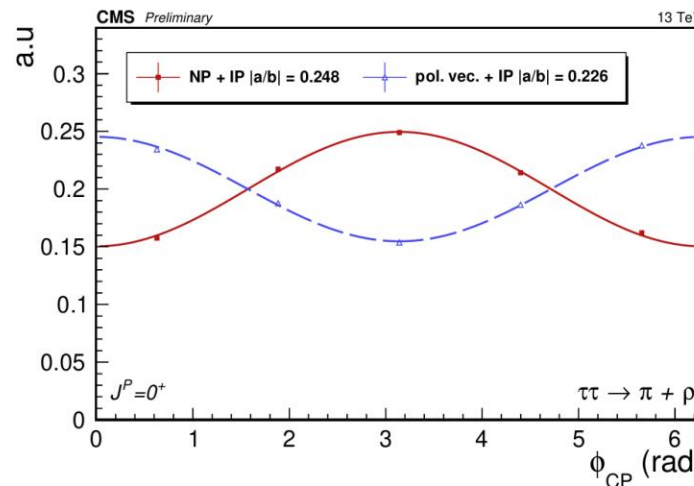
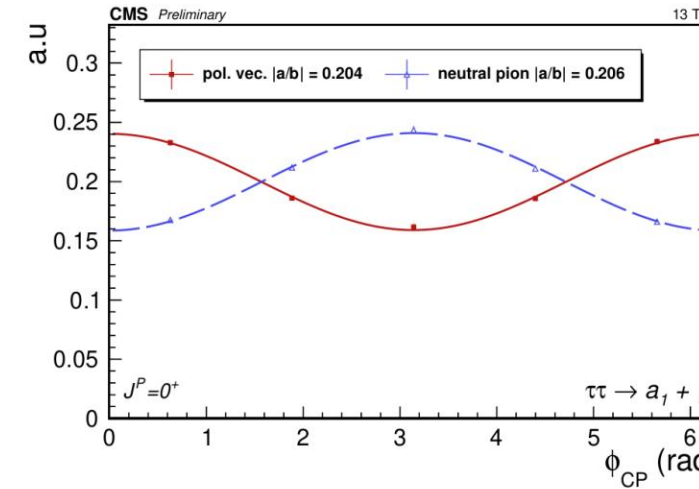
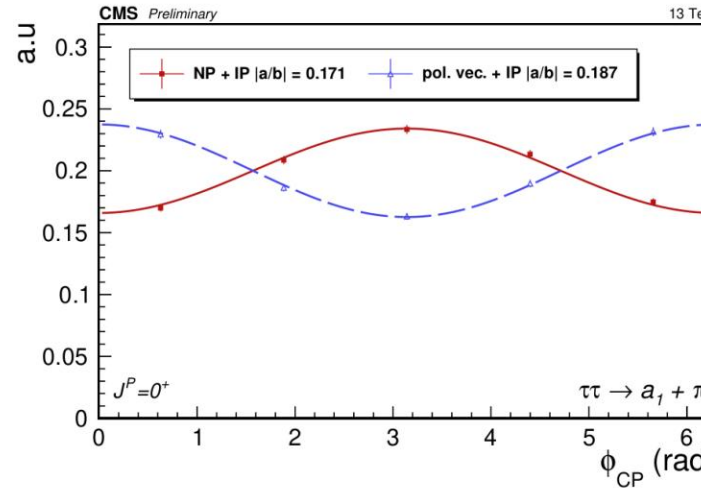
$H/Z \rightarrow \tau\tau$ by kinematic adjustment in
 $\tau \rightarrow a_1\nu$ (SV-PV)

$$|\vec{p}_\tau| = \frac{(m_{a_1}^2 + m_\tau^2)|\vec{p}_{a_1}| \cos \theta_{GJ} \pm \sqrt{(m_{a_1}^2 + \vec{p}_{a_1}^2)((m_{a_1}^2 - m_\tau^2)^2 - 4m_\tau^2 \vec{p}_{a_1}^2 \sin^2 \theta_{GJ})}}{2(m_{a_1}^2 + \vec{p}_{a_1}^2 \sin^2 \theta_{GJ})} \quad (6.17)$$



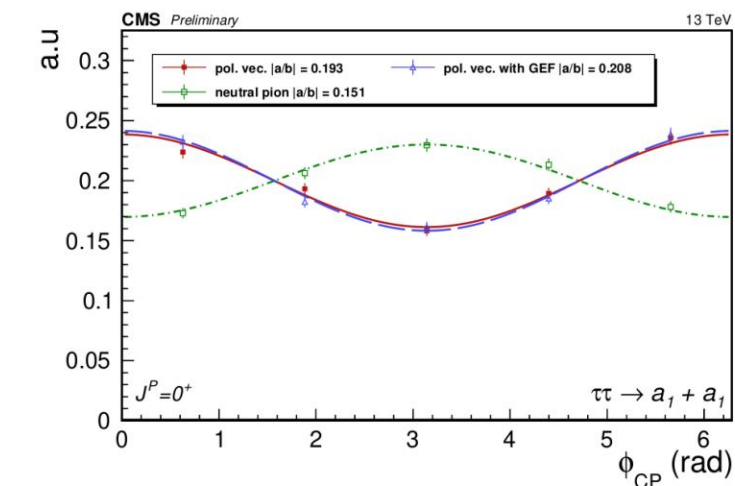
Polarimetric vector performance

reconstructed level



- Taus reconstructed from the best component of each algorithm

$$P_\tau = (\|\vec{P}_{SVfit}\| \times \vec{n}_{FastMTT}, E_{SVfit})$$

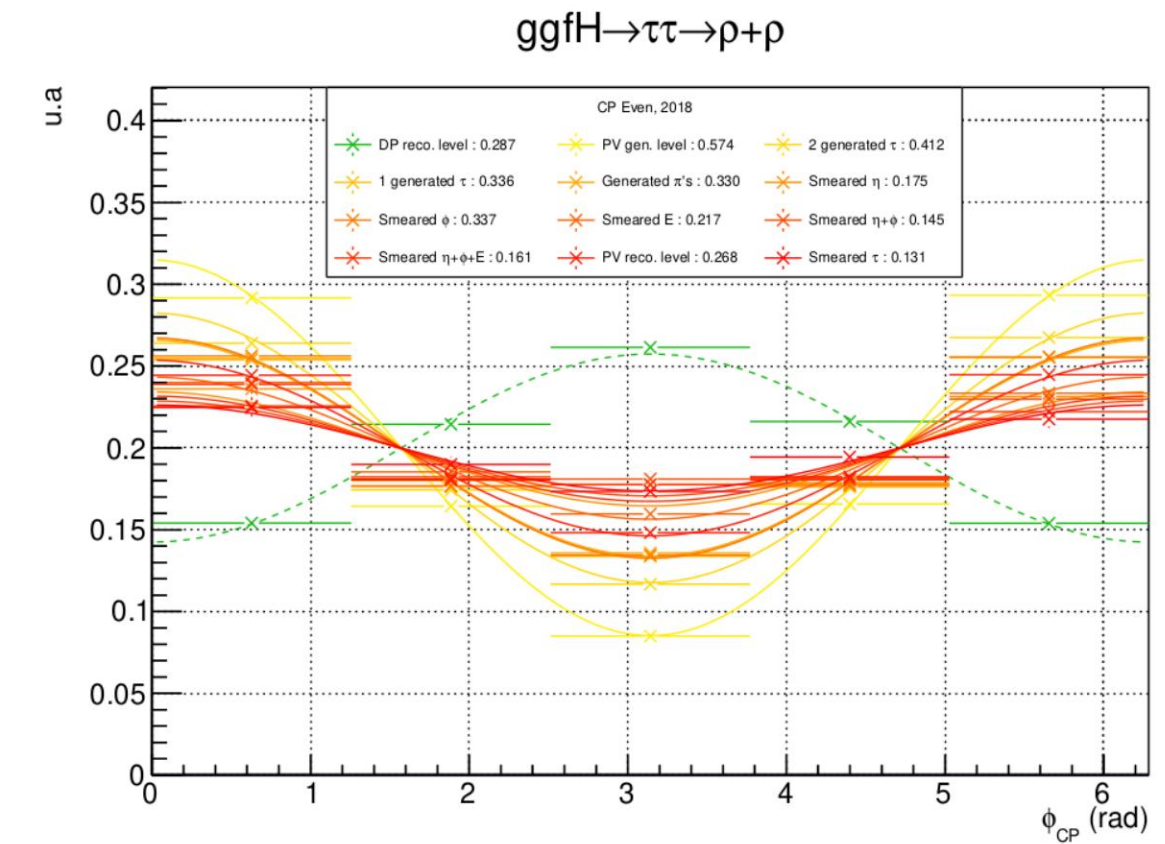


Polarimetric vector performance

conclusion



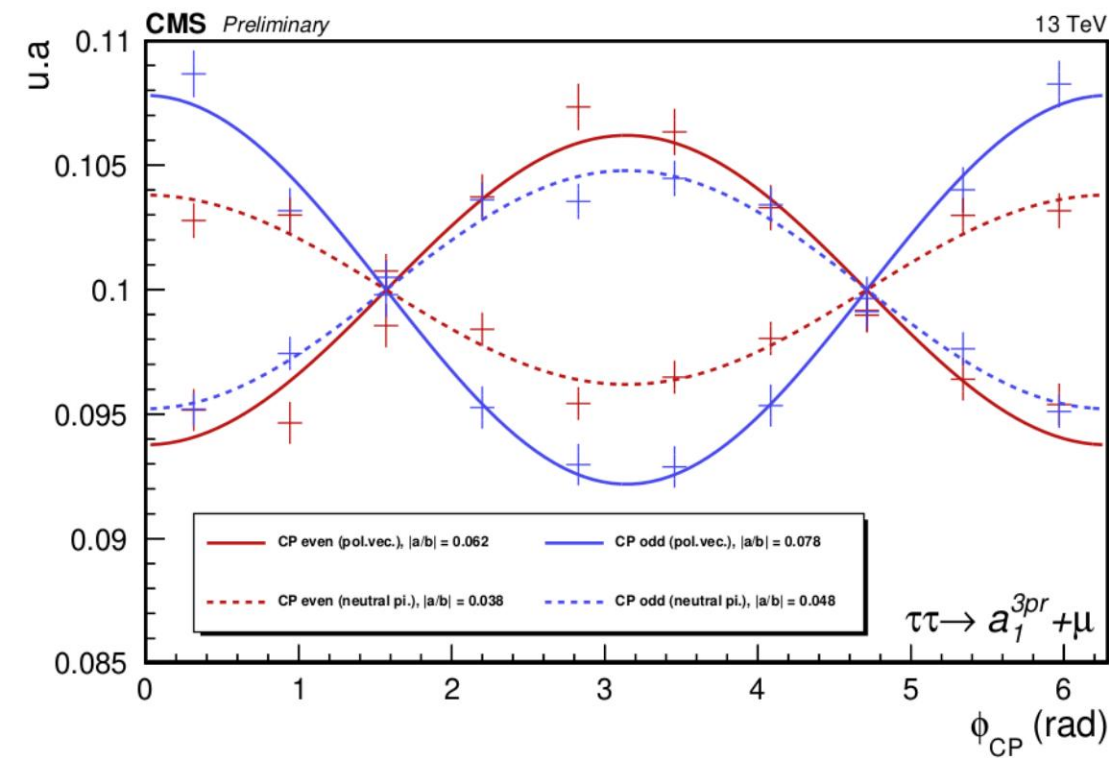
- Potential improvement thanks to the vp on rho hadronic decays and a1
- Impact parameter method to keep
- Introduction of a progressive degradation of the impulse components
 - The amplitude seems to be strongly correlated with the quality of the reconstruction of the angular components





Measurement in channel $a_1 + \mu$

- Taus reconstructed with GEF
- Amplitude improvement ~60% with the polarimetric vector vs decay plane





Measurement in channel $a_1 + \mu$

- Pair selection criteria

$\tau_h\mu$:

Muon :

- $p_T > 20 \text{ GeV}$ et $|\eta| < 2,4$,
- $d_z < 0,2 \text{ cm}$ et $d_{xy} < 0,045 \text{ cm}$,
- Identifié au point de fonctionnement *Medium* du Muon ID,
- Isolement relatif $< 0,15$.

Tau hadronique :

- $p_T > 20 \text{ GeV}$ et $|\eta| < 2,3$,
- $d_z < 0,2 \text{ cm}$,
- Mode de désintégration HPS $\in \{0, 1, 2, 10, 11\}$,
- Identifié au point de fonctionnement *Medium* de DeepTau vs Jets,
- Identifié au point de fonctionnement *VVLoose* de DeepTau vs Electrons,
- Identifié au point de fonctionnement *Tight* de DeepTau vs Muons.

- At least one trigger system path

- “SingleMuon”: presence of an isolated muon
- “TauXMuon”: presence of an isolated muon and a hadronic tau



Measurement in channel $a_1 + \mu$

- Estimation of background noise:

- $Z \rightarrow \tau\tau$: *embedded samples*
- Electroweak processes, VV, top quarks, $Z \rightarrow \ell\ell (\ell \neq \tau)$: MC simulation
- $jet \rightarrow \tau_h$ (QCD, W+jets, pair of tops): Fake Factors method

- Fake Factors:

$$FF_i = \frac{N(\text{Medium})}{N(\text{VVVLoose} \ \&\& \ !\text{Medium})},$$

$$\overline{FF} = \sum_i f_i \cdot FF_i, \quad \text{with} \quad f_i = \frac{n_i}{\sum_j n_j},$$

- Calculation of FF in a region enriched with “false” taus
- Application of FFs in the region (VVVLoose $\&\&$!Medium)

- Classification of events with a BDT (QCD, W+jets, pair of tops)

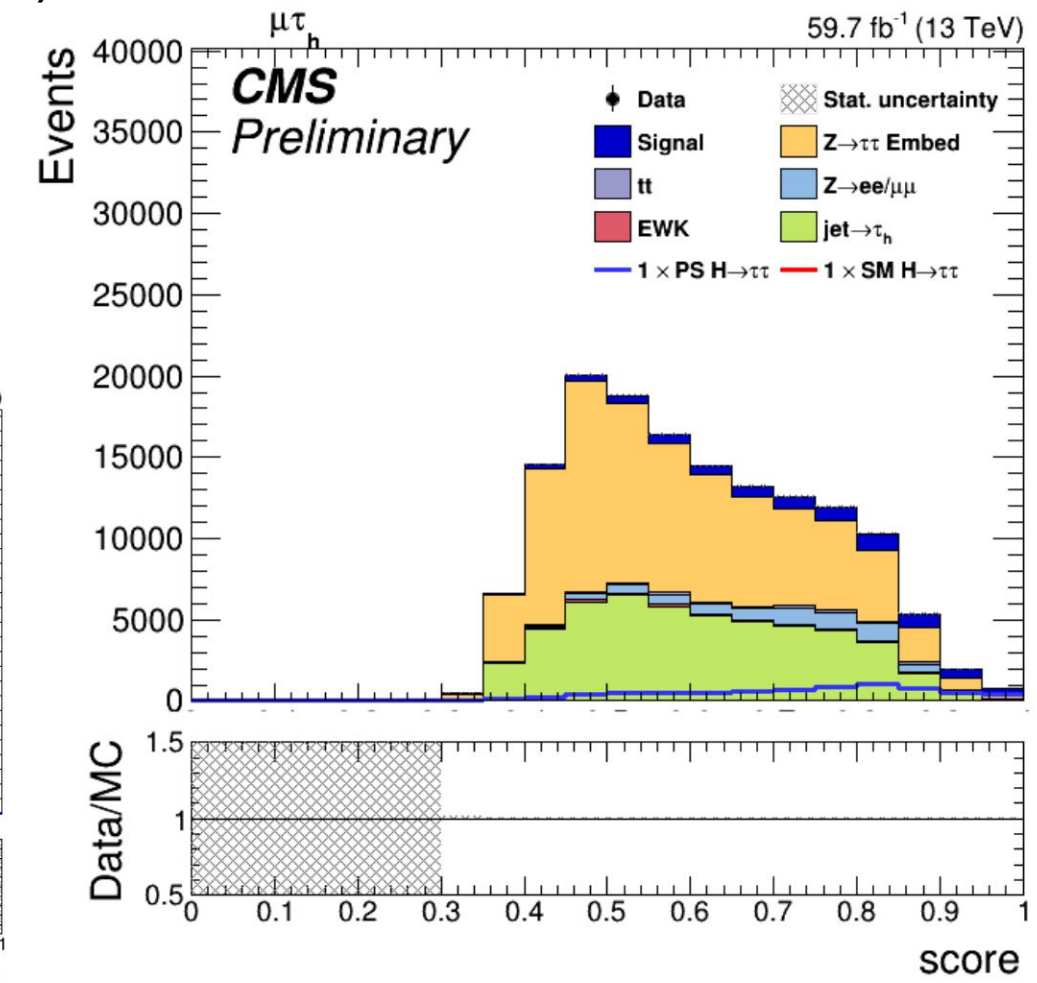
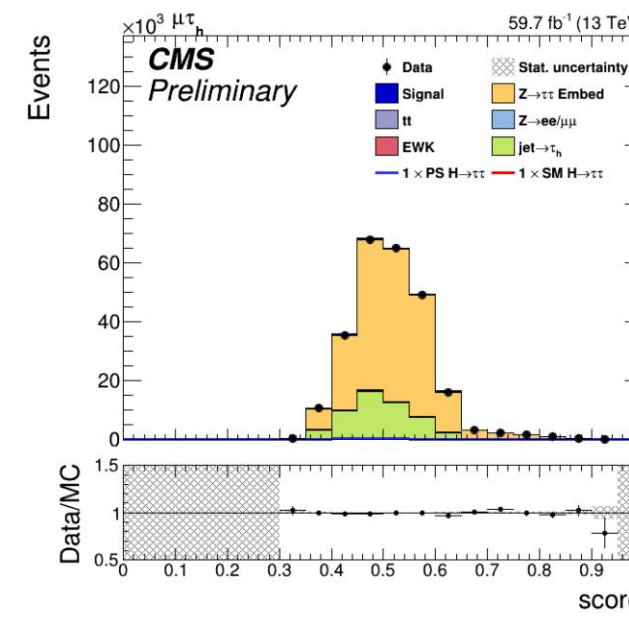
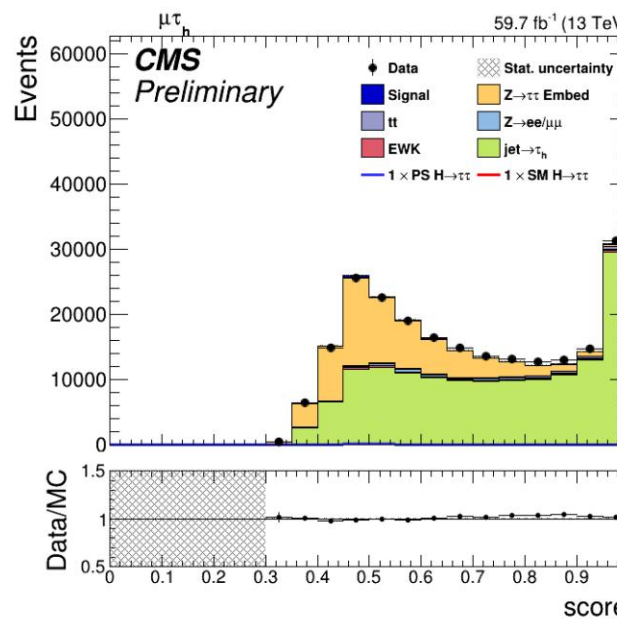


Measurement in channel $a_1 + \mu$

- Categorization by a multi-class BDT (XGBoost)

- Higgs (signal)
- ZTT embedded (real taus)
- JetFakes (fake taus)

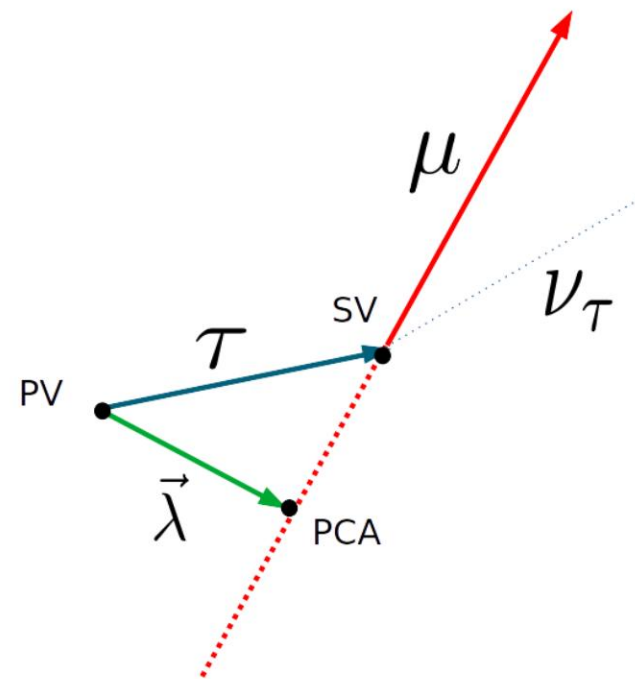
- Training in 2018



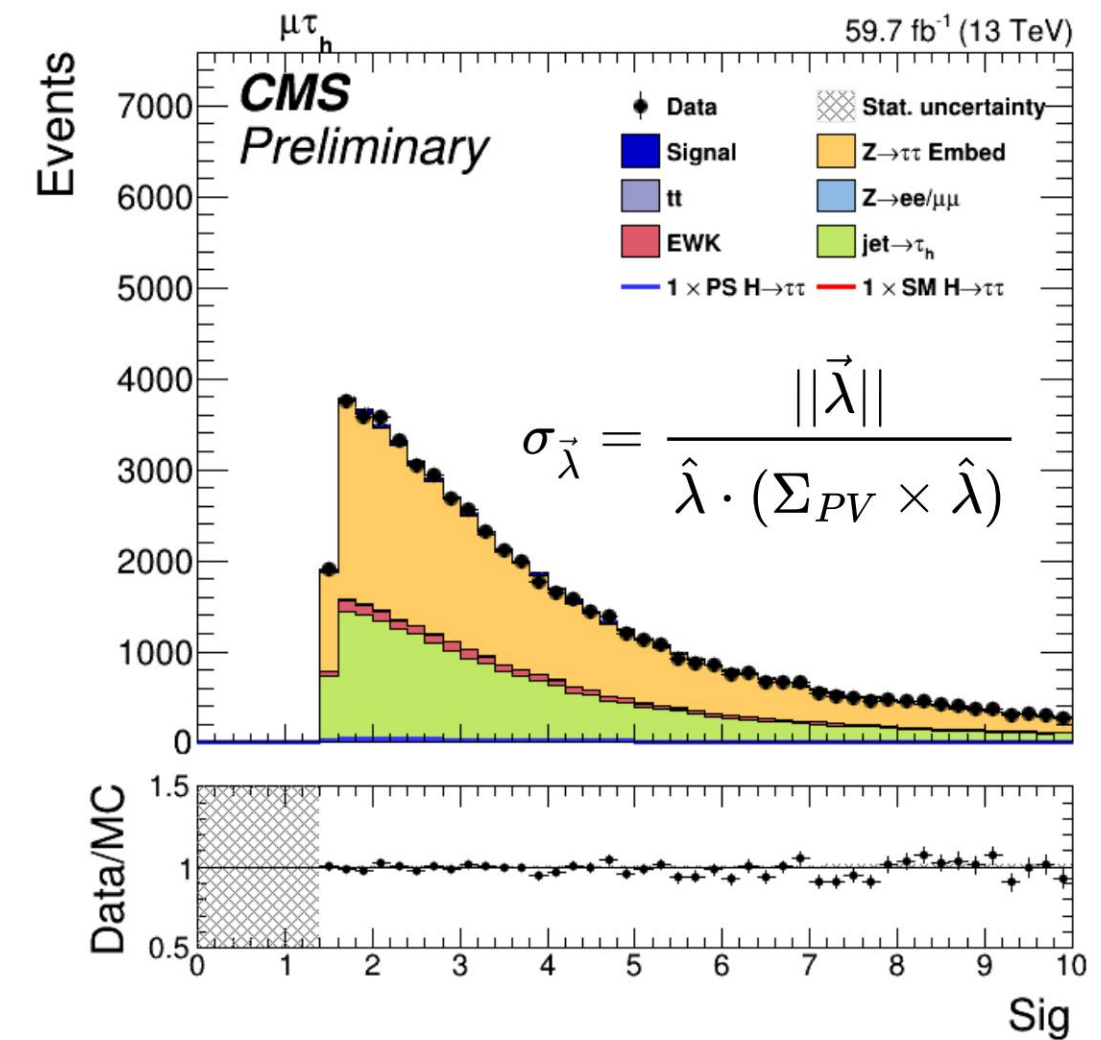
Measurement in channel $a_1 + \mu$



- Impact parameter: linear extrapolation



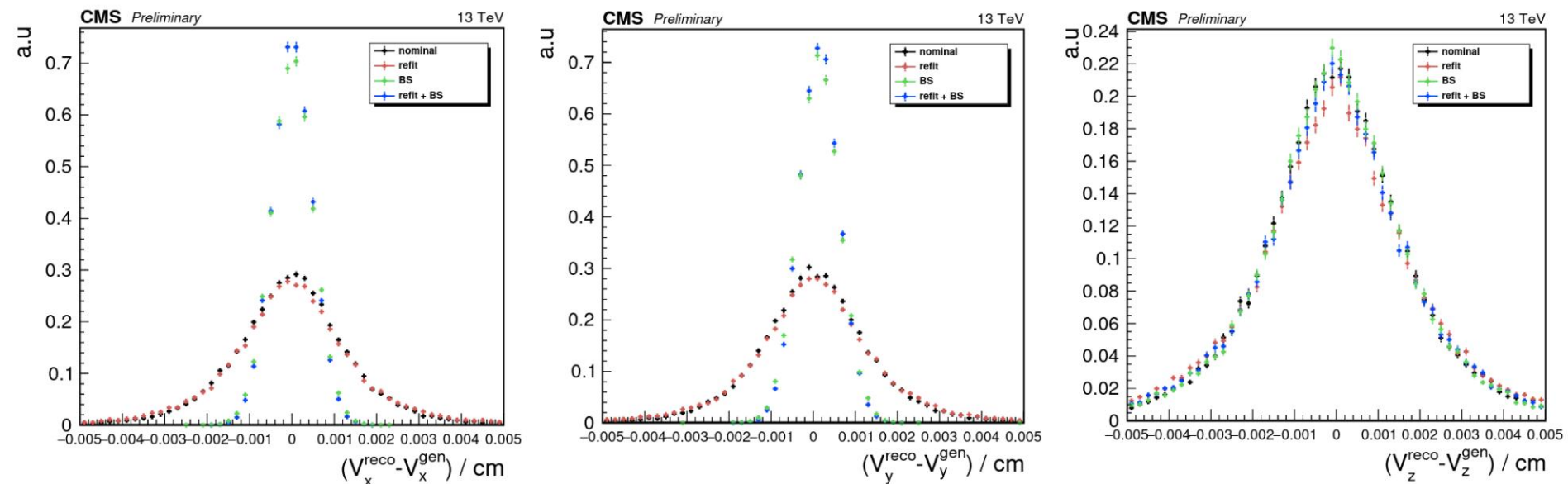
- Correction of coordinates by “quantile mapping”
- Cutoff on significance >1.5





Measurement in channel $a_1 + \mu$

- Choice of primary vertex
 - Nominal: calculation from all traces associated with the PV
 - Refit: traceless adjustment of tau leptons
 - BS: adjustment with constraint on the position of the beamspot
- In this analysis: refit + BS





Measurement in channel a1+ μ

- Adjustment model:

$$L(\alpha^{H\tau\tau}, \mathcal{B}^{\tau\tau} = 1, \mu_{ggH}, \mu_V, \vec{\theta}) = \prod_j^{N_{\text{cats}}} \prod_i^{N_{\text{bin}}^j} P\left(n_{i,j} | S_{i,j}(\alpha^{H\tau\tau}, \mathcal{B}^{\tau\tau} = 1, \mu_{ggH}, \mu_V, \vec{\theta}) + B_{i,j}(\vec{\theta})\right) \times \prod_m^{N_{\text{nuis}}} C_m(\theta_m | \tilde{\theta}_m), \quad (7.8)$$

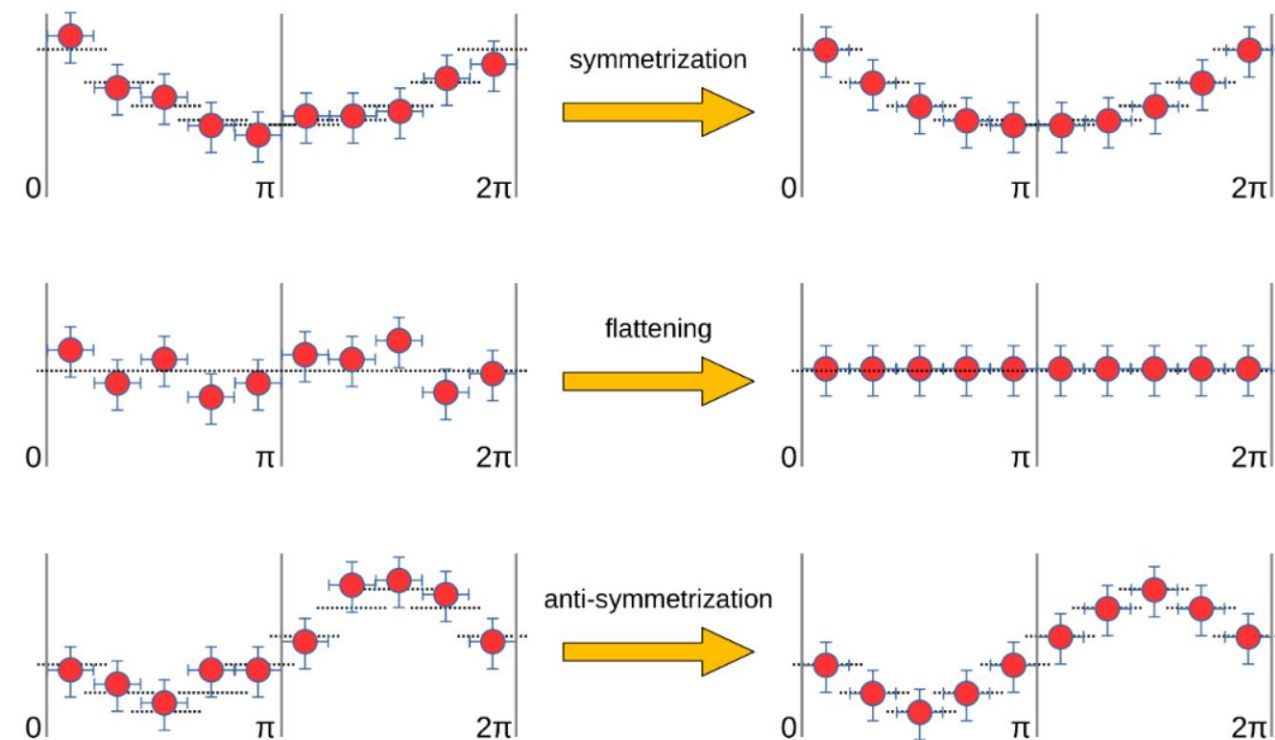
- Probability (Poisson) of obtaining n events with S signal events and B expected background noise events
- Weighting by C_m nuisance parameters
- Log-likelihood minimization

$$NLL = -\log(L(\alpha^{H\tau\tau}, \mathcal{B}^{\tau\tau} = 1, \mu_{ggH}, \mu_V, \vec{\theta})),$$



Measurement in channel $a_1 + \mu$

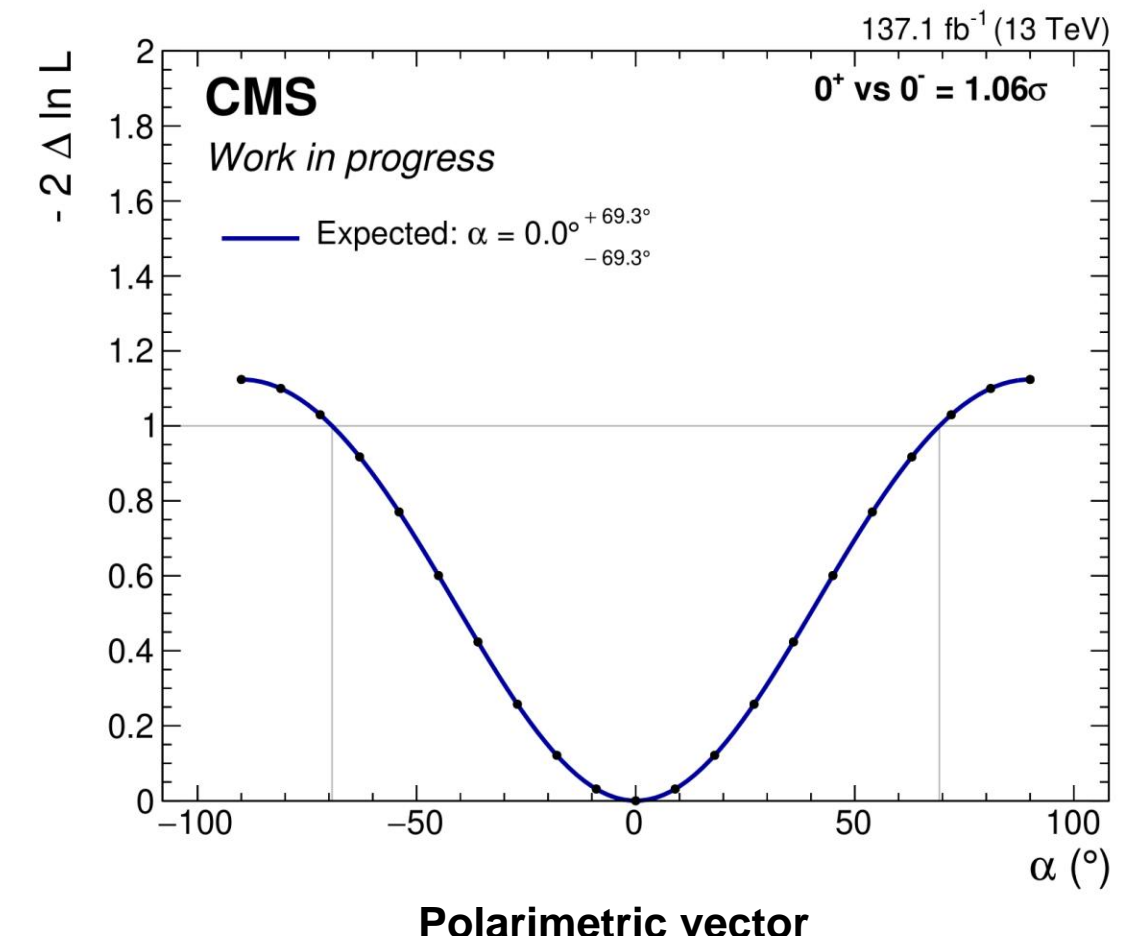
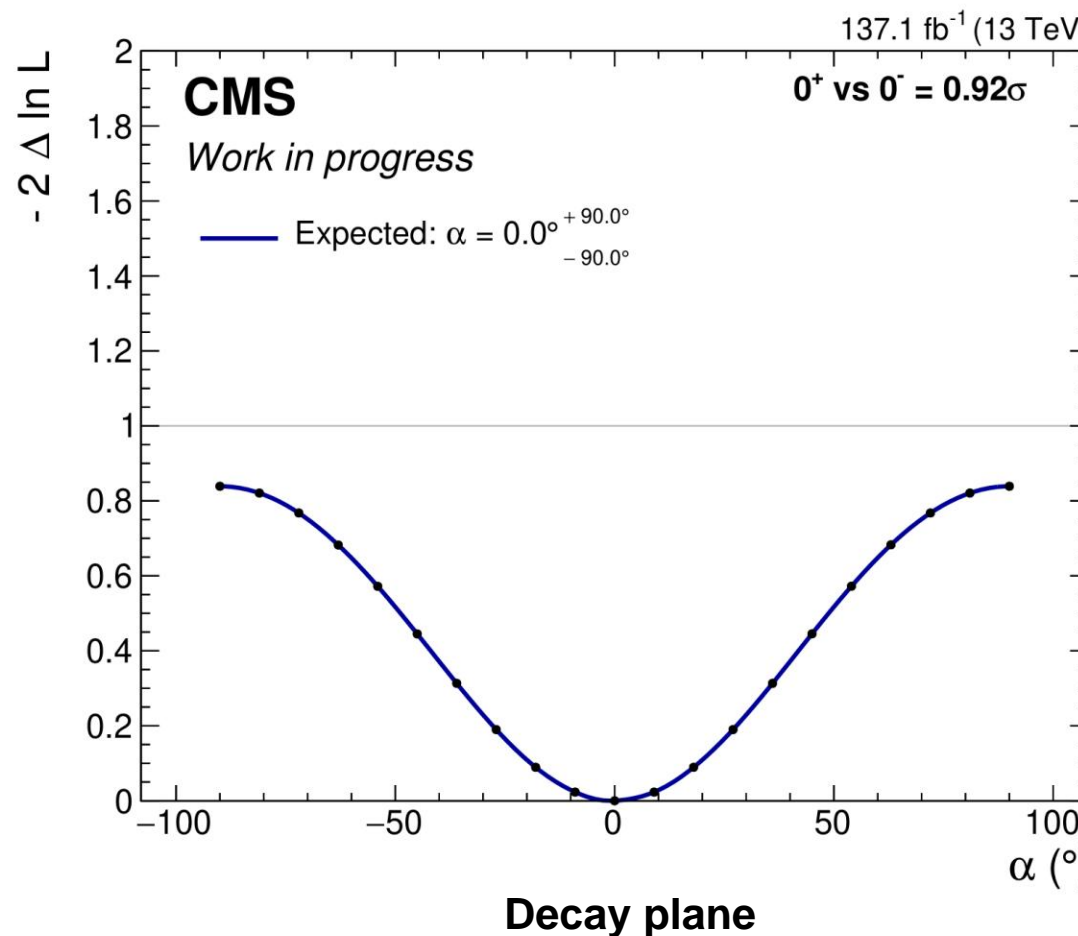
- Smoothing procedure:
 - Signal, jet fakes: symmetrization of distributions around π by pairs of bins
 - Other background noise: flattening at the mean value of the distribution





Measurement in channel $a_1 + \mu$

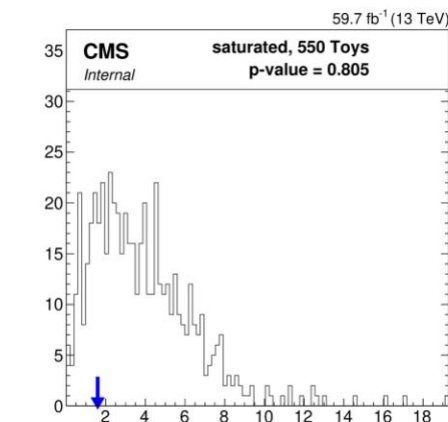
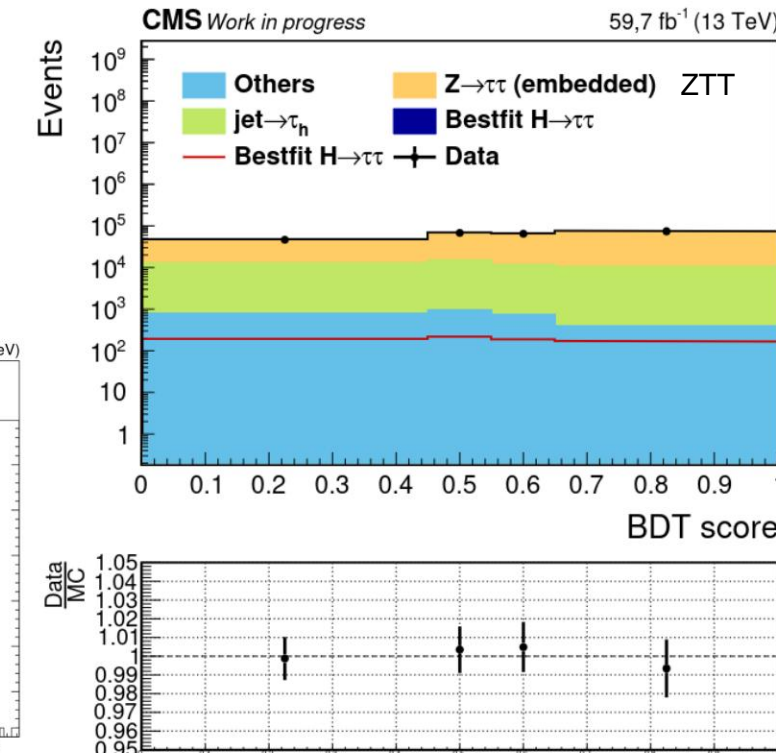
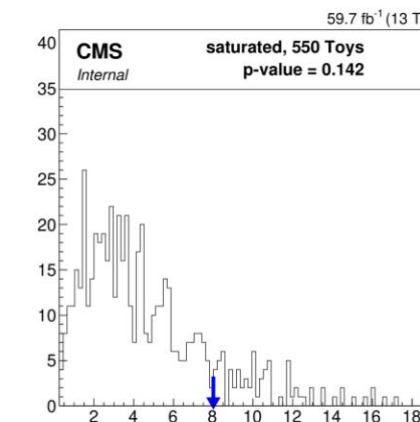
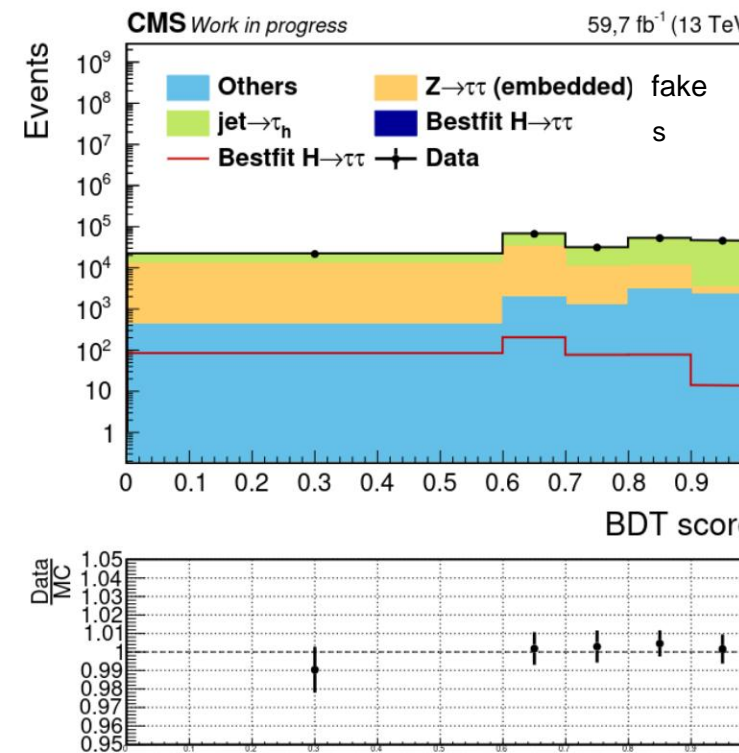
- Expected results: +15% polarimetric vector sensitivity vs plane decay





Measurement in channel $a_1 + \mu$

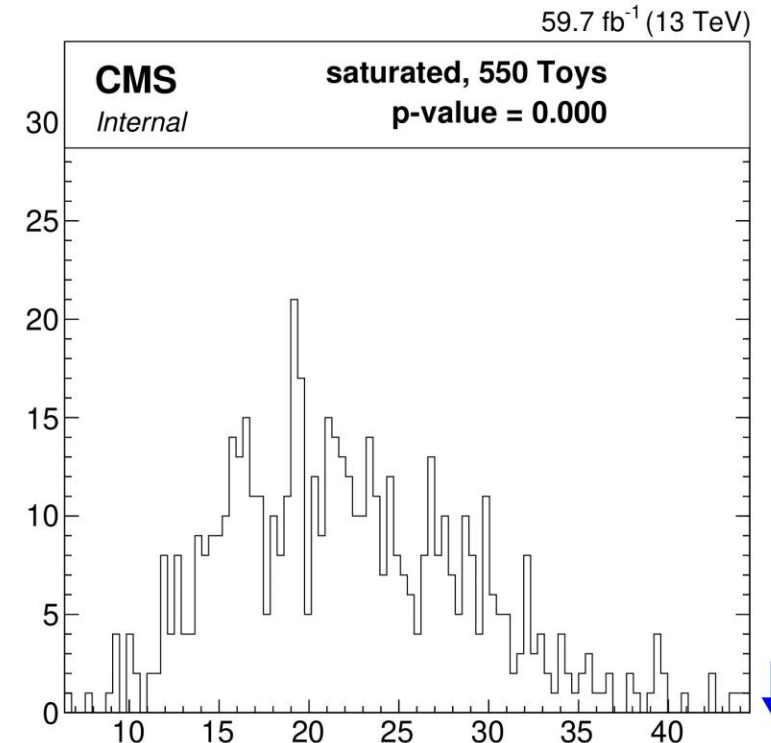
- Data unblinding procedure for 2018:
 - Background noise categories ($\bullet \tau_h \mu$)
 - Data/MC agreement (post fit) and saturated GOF





Measurement in channel $a_1 + \mu$

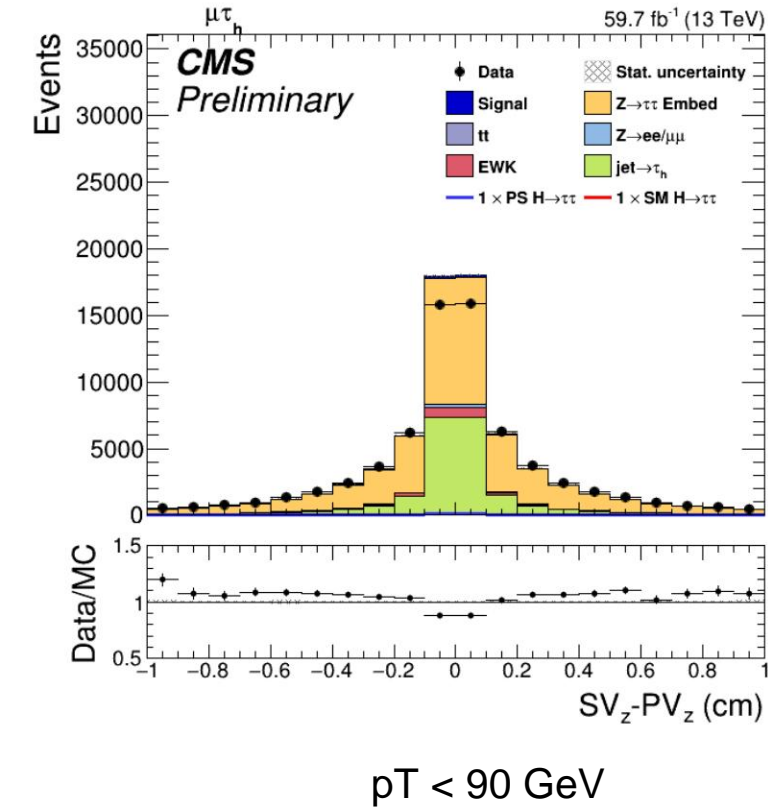
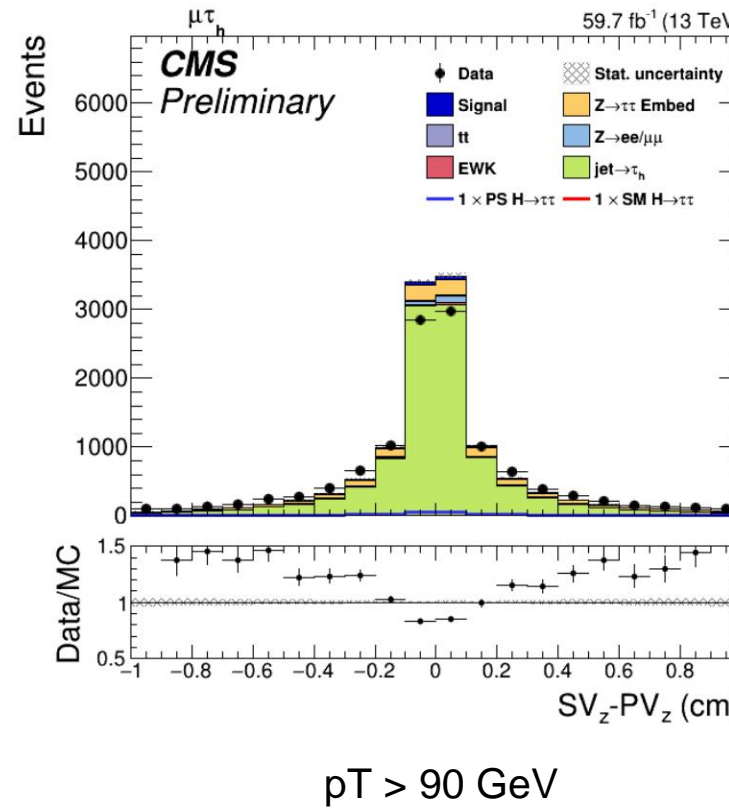
- Data unblinding procedure for 2018:
 - Signal category ($a_1 + \mu$) with the polarimetric vector
 - zero p-value, stop of the unblinding procedure





Measurement in channel $a_1 + \mu$

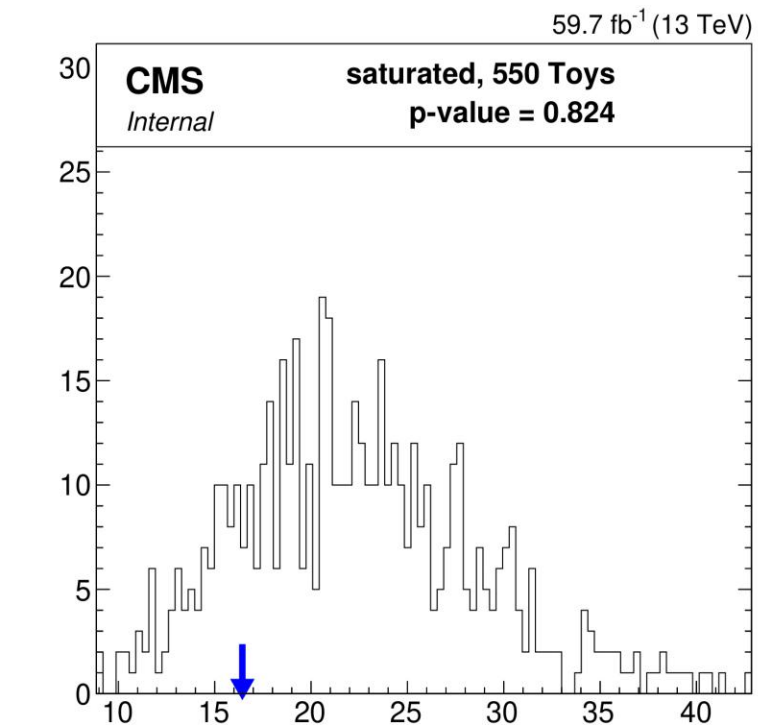
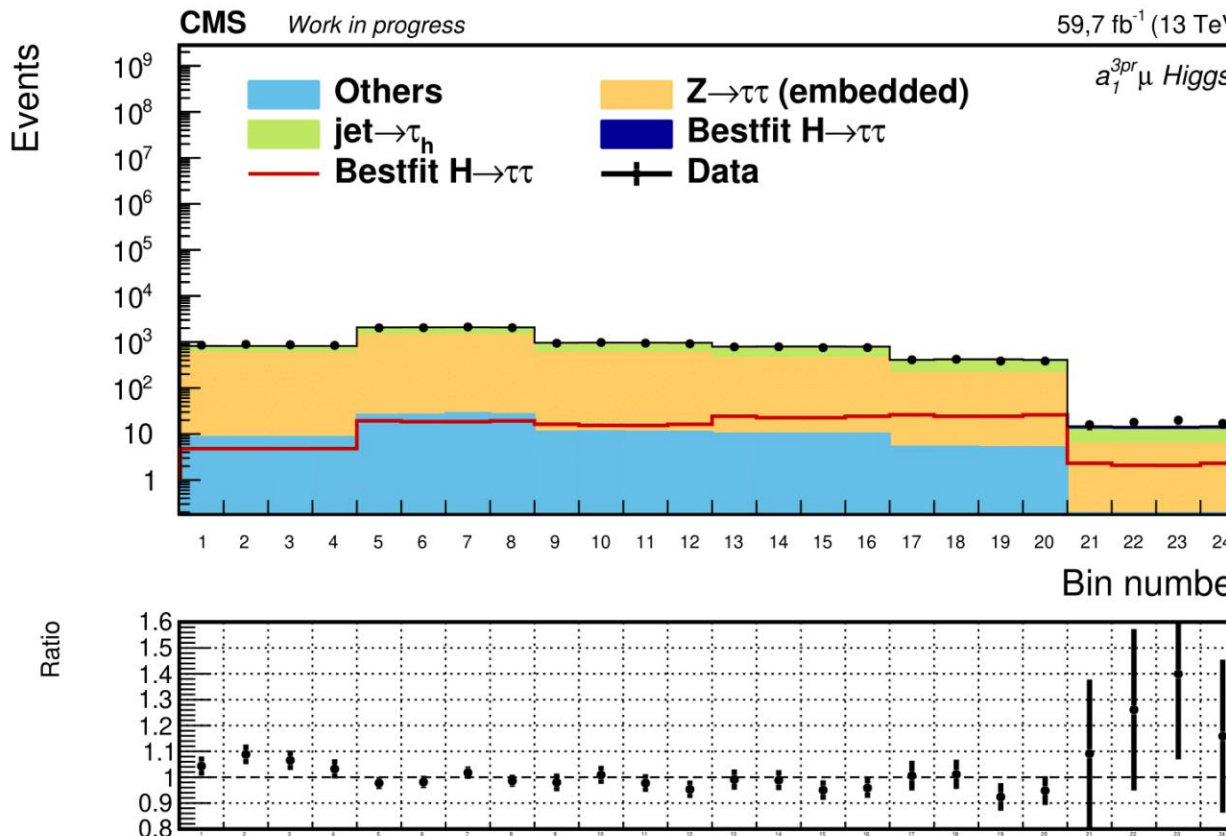
- Modeling error of the secondary vertex in the region $pT > 90$ GeV
 - Used only by the GEF algorithm for the polarimetric vector method





Measurement in channel $a_1 + \mu$

- Unblinding data 2018 decay plane
 - Signal category ($a_1 + \mu$) postfit





Conclusion and prospects

- This thesis presents a study of the performance of the polarimetric vector method for the analysis of the CP properties of the Yukawa coupling of the tau lepton
 - Used in channel $a_1 a_1$ only to date
 - Possible improvement in decays $\tau \rightarrow \rho, a_1$
- Presentation of an analysis in the $a_1 + \mu$ channel
 - Expected sensitivity improvement of 15% in Run 2 data
- Run 3:
 - New tau reconstruction algorithms
 - Deployment of the polarimetric vector method

